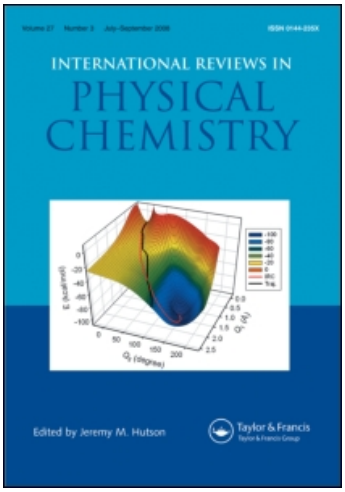

International Reviews in Physical Chemistry
Publication details, including instructions for authors and subscription information:
http://www.informaworld.com/smpp/title~content=t713724383

Novel quasi-aromatic transition metal cluster compounds

Jia-Xi Lu[a]; Zhi-Da Chen[a]
[a] Fujian Institute of Research on the Structure of Matter, Chinese Academy of Sciences, State Key Laboratory of Structural Chemistry, Fuzhou, Fujian, PR China

To cite this Article Lu, Jia-Xi and Chen, Zhi-Da(1994) 'Novel quasi-aromatic transition metal cluster compounds', International Reviews in Physical Chemistry, 13: 1, 85 — 121
To link to this Article: DOI: 10.1080/01442359409353291
URL: http://dx.doi.org/10.1080/01442359409353291

INTERNATIONAL REVIEWS IN PHYSICAL CHEMISTRY, 1994, VOL. 13, NO. 1, 85–121

Novel quasi-aromatic transition metal cluster compounds

by JIA-XI LU and ZHI-DA CHEN

Fujian Institute of Research on the Structure of Matter,
Chinese Academy of Sciences, State Key Laboratory of
Structural Chemistry, Fuzhou, Fujian, PR China 350002

From the point of view of chemical reactivities, molecular configurations, and bonding characteristics, a series of novel quasi-aromatic transition metal cluster compounds has been studied in this article. Experimental evidences for the cluster compounds $[M_3(\mu_3\text{–}X)(\mu\text{–}Y)_3]^{4+}$ (M = Mo, W; X, Y = O, S, Se, Te) containing a puckered $\{M_3(\mu\text{–}Y)_3\}$ six-membered rings reveal benzene-like structural characteristics and chemical behaviours in a series of ligand substitution, addition, and oxidation reactions. The energy localized CNDO/2 molecular orbital method is applied to elucidate the nature of quasi-aromaticity in this type of cluster compound. The localized molecular orbitals (LMOs) of benzene as an aromatic prototype and a series of planar monocyclic polyene hydrocarbons $C_nH_n^q$ as well as certain typical conjugated six-membered rings are investigated, leading a deep-rooted inherent relationship between their aromaticity and bonding characteristics. The LMO analyses for these cluster compounds with $[Mo_3(\mu_3\text{–}X)(\mu\text{–}Y)_3]^{4+}$ show that in both benzene and such cluster compounds there exists a closed, smoothly continuous conjugated π-electron system, formed from three synergistically connected three-centred two-electron π bonds, which is a (p–p–p)π conjugated system in the former, but a (d–p–d)π one for the latter. The size and electronegativity of the bridging atom (μ–Y) affect significantly the degrees of quasi-aromaticity in these cluster compounds with the core $[M_3(\mu_3\text{–}X)(\mu\text{–}Y)_3]^{4+}$ (Y = O, S, Se, Te); on the other hand, the stronger interaction between the metal atom M and the terminal ligands with lone-pair electrons results in a smaller quasi-aromaticity of the puckered $[M_3Y_3]$ ring. The bonding patterns of the cubane-type $[Mo_3S_4ML_2]^{(4+q)+}$ and the sandwich-type $[Mo_3S_4MS_4Mo_3]^{8+}$ formed from the quasi-aromatic ligand $[Mo_3S_4]^{4+}$ with a metal atom M are discussed in detail. Finally, criteria have been formulated for the formation of a closed, smoothly continuous π-conjugated system in these $[M_3Y_3]$ rings.

1. Introduction

Faraday discovered benzene in 1825 in the condensate of an illuminating gas obtained in the pyrolysis of whale oil. This important discovery was then followed in 1865 by the proposal of the famous chemical structural formula for benzene by Kekulé and the introduction of the concept of 'aromaticity' for the description of chemical structural characteristics of benzene-like compounds related to benzene. This concept of aromaticity has since then become a very valuable and useful one, and played an important role in the advancement of organic chemistry. So far, this new concept has widely pervaded numerous areas of organic as well as inorganic chemistry, in the former case particularly in the discovery and synthesis of its derivatives, such as monocyclic, heterocyclic, polycyclic, monoaromatic systems and also annulenes and numerous aromatic transition states. In the field of inorganic chemistry, there are, for example, metallocenes and a variety of inorganic conjugated rings and heterocyclic systems containing metal atoms [1]. On the other hand, the recent upsurge of interest in aromaticity has been further triggered by the structural characteristics and unusual

0144–235X/94 $10·00

stability of the fullerene family, each member of which can be regarded as a pseudospherical molecule with a round hollow cage structure [2]. Thus, on the surface of the C_{60} fullerene, there are 20 six-membered carbon rings and 12 five-membered carbon rings. A general description of bonding for this pseudospherical cluster, based on a qualitative molecular orbital theory, assumes that each carbon atom contributes three tangential sp^2 hybridized orbitals to the network of single bonds along the polyhedral edges. This then leaves a radial p orbital on each vertex available for delocalized 'π bonding', which distributes π electrons around the whole pseudospherical face. Hence the world of coplanar polycyclic aromatic chemistry is now augmented by the addition of these new π systems with pseudospherical frameworks. In this paper, we shall give a brief review of another novel type of aromatic compounds, which exists in the puckered $[Mo_3S_3]$ six-membered rings in certain trinuclear molybdenum cluster compounds with the $[Mo_3(\mu_3\text{-}S)(\mu_2\text{-}S)_3]^{4+}$ cores. It should be noted that this type of aromatic compounds in transition metal cluster chemistry is indeed an interesting and intriguing addition in aromatic chemistry.

The usefulness of the concept of aromaticity, as mentioned above, resides in its generality, which reflects, in fact, a real physical phenomenon, associated with the presence of an odd number of π-electron pairs interacting in an approximately planar ring with continuous conjugation. However, a drawback of the initial proposal of this concept is that it does not admit of any quantitative measurement of its aromaticity. Therefore, with further developments in aromatic chemistry as well as in novel types of aromatic compounds, some criteria must be formulated for the classification of compounds as aromatic against non-aromatic. So far as the original concept of aromaticity proposed by Kekulé is concerned, it is necessary to relate structural characteristics of compounds with those of benzene in regard to their cyclic π conjugation. Immediately afterward, Erlenmayer proposed in 1866 that the concept of aromaticity should also be associated with chemical reactivity. Thus it should be noted that another historical landmark in aromatic chemistry must be credited to Hückel, who proposed the first crude, quantum-chemical model for aromatic compounds and 'derived' thereby the 'magic $(4n+2)$' π-electron rule [3]. A suitable definition on this basis would be that aromatic systems are monocarbocyclic, continuous conjugated molecules containing $(4n+2)$ out-of-plane π electrons. However, this would have the disadvantage of excluding those compounds such as thiophene, pyridine and naphthalene, etc. as being aromatic. This difficulty is even apparent in monocyclic systems both with regard to certain non-bonding interactions and an upper limit on the size of the ring, and therefore a satisfactory definition of aromatic compounds would have to be placed on the value of n. Furthermore, it should be pointed out that Ingold, Pauling, Wheland and M. J. S. Dewar have defined an aromatic molecule as a cyclic system having a larger resonance energy in which all the atoms in this ring take part in a single continuous conjugated system [4]. This definition in terms of the additional thermodynamic stability of a molecule over that predicted on the basis of a localized two-electron bond model, although very satisfactory in principle, is difficult to apply in practice because the resonance energy is a difficult parameter to theoretically define and measure. A more plausible approach to this aromaticity problem therefore calls for the consideration of physical properties such as induced ring current, Faraday effect, diamagnetic susceptibility exaltation, tendency towards bond equalization, and first and second-order bond fixation. It is clear that all these additional properties have the advantage that they are easily measurable, but unfortunately they seldom give consistent results among themselves.

As mentioned above, both theoretical and experimental approaches to the classification of compounds as aromatic against non-aromatic have advantages and disadvantages. It is believed that the concept of aromaticity, reflecting a real physical phenomenon associated with the π-electron delocalization of cyclic molecules, must take into consideration multiple structural, chemical and physical manifestations. Therefore, attempts to relate a particular aspect of these phenomena to the degree of aromaticity can only be fraught with difficulty. In this paper, we shall stress the phenomena involved in structural characteristics, chemical reactivities, electronic structural features and other physical properties for novel types of quasi-aromatic cluster compounds.

Following the development of cluster chemistry of boranes and carboranes, a period of extensive research and development came into existence in the field of transition metal cluster chemistry. During the past decade, the chemistry of metal–metal bonded trinuclear metal cluster compounds, especially those containing Mo and W, has been rapidly expanded [5–11]. This allows us to study systematically structural characteristics, chemical reactivities, electronic structural features and other physical properties for this trinuclear Mo and W cluster compounds. The following parent Mo–S cluster: $[Mo_3(\mu_3\text{–}S_c)(\mu_2\text{–}S_b)_3(\mu_2\text{–dtp})(\chi\text{–dtp})_3(OH_2)]$ (I) (figure 1) containing a puckered $[Mo_3(\mu_2\text{–}S)_3]$ six-membered ring, where dtp denotes $\{S_2P(OEt)_2\}^{-1}$, and S_c, S_b, and χ denote the capping S atom, the bridging S atoms and the chelating dtp ligands respectively, exhibit obviously benzene-like chemical behaviour and structural characteristics [12]. Indeed, this strange phenomenon aroused our interest in the discussion of its possible aromaticity in transition metal cluster chemistry [13, 14]. In this article we will describe this novel type of quasi-aromatic cluster compounds in transition metal cluster chemistry and its chemical and physical properties, as well as their electronic structures. It should be pointed out that in so far as quasi-aromaticity in cluster chemistry is concerned, both the cluster core itself and the cluster ligands must be taken into detailed consideration. It is beyond doubt that there exist benzene-like behaviours, which will be stressed herein, as well as benzene-unlike behaviours, which would not be discussed in detail here for the time being.

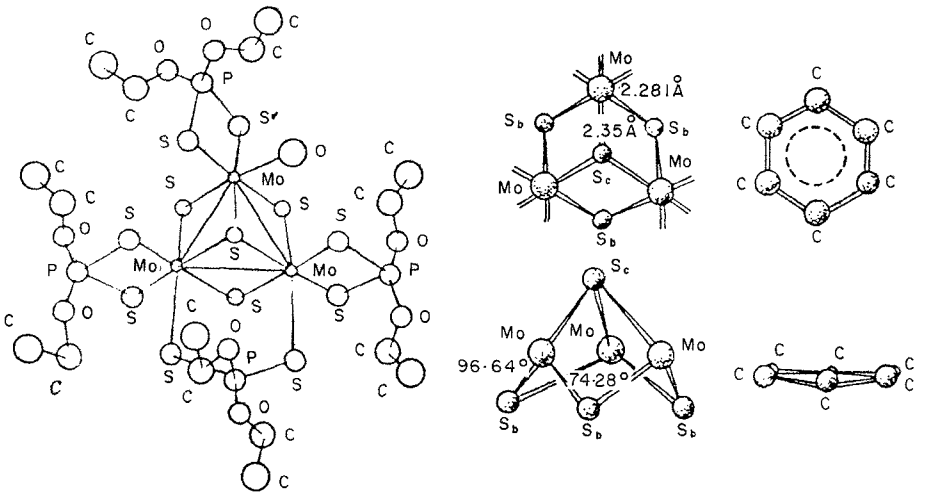

Figure 1. Molecular configuration of the cluster molecule $[Mo_3(\mu_3\text{–}S)(\mu_2\text{–}S)_3(\mu_2\text{–dtp})(\chi\text{–dtp})_3(OH_2)]$ (dtp = $[S_2P(OEt_2)^-]$) and quasi-aromaticity of the puckered $[Mo_3S_3]$ ring as the most essential part of the $[Mo_3S_4]^{4+}$ core. H atoms are not shown.

2. Localized molecular orbitals of typical aromatic compounds

As was indicated in the previous Section, the history of the development of aromatic chemistry is fraught with fruitful interactions between experiments and theories. Many of the original ideas have been later modified. However, many have been generally accepted and the interplay of experimental investigations and theoretical considerations still continues to be fruitful in this area, leading to the synthesis of new aromatic compounds and the formulation of new theoretical concepts. It should be noted that the modern molecular orbital theoretical method plays an important role in the advancement of aromatic chemistry. However, the canonical molecular orbitals (CMO) calculated from molecular orbital theoretical methods under various approximations imply in principle a delocalization description for the electronic structure of the cluster molecule, and yet it is rather difficult to explore the delocalizability of π electrons in these aromatic molecules. It is well known that the molecular structure of benzene cannot be described in term of a single Kekulé structural formula alone. This fact has certainly a deep-rooted inherent relationship to aromaticity. Then what are the localized molecular orbitals for benzene? We believe that the delocalizability of π electrons in the benzene molecule can be best understood in terms of localized molecular orbitals (LMOs). Several localization techniques recently developed on the basis of linear combination of atomic orbitals-self-consistent field-molecular orbital (LCAO-SCF-MO) approximate methods have enabled us to make use of them in the study of delocalizability of electronic structures in aromatic or quasi-aromatic molecules. In this and later Sections, a reasonable quantum-chemical picture of the various bonds in aromatic or quasi-aromatic cluster molecules is obtained by the use of Edmiston–Ruedenberg energy-localized MOs [15, 16] calculated under the spin-unrestricted complete neglect of differential overlap (CNDO)/2 approximation, and compared with pseudopotential *ab initio* calculations followed by the Boys' localization method [17], so as to arrive at a deeper insight into the nature of quasi-aromaticity. It is worth pointing out that Lipscomb has successfully described the characteristics of the electron distributions in boranes and carboranes by the use of localized molecular orbital method leading to the formulation of three-centred bonds in such electron deficient molecules [18]. It is obvious from our theoretical investigations that three-centred σ bonds involved therein represent only one type of three-centred bonds, whereas another type of three-centred π bonds will be shown to exist as well.

2.1. *Energy-localized approach* [15, 18]

For a closed-shell state of a molecule, when the Hamiltonian operates on a single determinant wavefunction constructed from molecular orbitals ϕ_i:

$$\mathscr{H}=\sum_i\left[-\tfrac{1}{2}\nabla^2(i)-\sum_A Z_A r_{Ai}\right]+\sum_{i>j} r_{ij}^{-1},$$

(in atomic units, for atoms A and electrons i), the total electronic energy is given by

$$E_0=2\sum_{i=1}^{n} H_{ii}+\sum_{i,j=1}^{n}(2J_{ij}-K_{ij}),$$

where the one-electron part is given by

$$E_1=2\sum_{i=1} H_{ii}=2\sum_{i=1}^{n}\int\phi_i(1)\left[-\tfrac{1}{2}\nabla^2(1)-\sum_A Z_A r_{Ak}\right]\phi_i(1)\,dv(1)$$

and the two-electron part

$$E_2 = \sum_{i>j} 4(ii|jj) - \sum_{i>j} 2(ij|ij),$$

is composed of Coulomb and exchange terms respectively, where

$$(ij|kl) = \int \phi_i(1)\phi_j(1) r_{12}^{-1} \phi_k(2)\phi_l(2)\, dv(1)\, dv(2),$$

on assuming only real orbitals. The molecular orbitals are usually expressed as linear combinations of atomic orbitals

$$\phi_i = \sum_p C_{pi}\psi_p,$$

where ψ_p are taken as Slater orbitals with Slater exponents ζ.

Minimization of the energy with respect to variation of the C_{pi}s, yields the SCF equations

$$FC = \varepsilon SC,$$

where $F = H$ (one-electron part) $+ G$ (two-electron part), S is the overlap matrix, and ε is in diagonal form. By the use of an iterative procedure one solves the secular determinant $|F - \varepsilon S| = 0$ for the εs and then the Cs.

Localization is approached by the unitary transformations of two orbitals at a time

$$\begin{cases} u_1 = \phi_1 \cos\theta + \phi_2 \sin\theta, \\ u_2 = -\phi_1 \sin\theta + \phi_2 \cos\theta, \end{cases}$$

where θ is not a real angle, but a parameter obtained by solving the following equations

$$A_{ij} = (\phi_i\phi_j|\phi_i\phi_j) - \tfrac{1}{4}(\phi_i^2 - \phi_j^2|\phi_i^2 - \phi_j^2),$$

$$B_{ij} = (\phi_i^2 - \phi_j^2|\phi_i\phi_j),$$

$$\theta = \tfrac{1}{4}\arctan(-B_{ij}/A_{ij}),$$

allowing the transformations to be written in the following unitary form:

$$\mathbf{F}^{\mathrm{LMO}} = \mathbf{U}^{\dagger}\mathbf{F}^{\mathrm{CMO}}\mathbf{U},$$

where $\mathbf{F}^{\mathrm{CMO}}$ and $\mathbf{F}^{\mathrm{LMO}}$ denote the Fock matrix of the canonical and localized MOs respectively, and $\mathbf{U}$ denotes the transformation unitary matrix. Consecutive pairwise transformations are carried out until

$$D = \sum_i (ii|ii),$$

is maximized, where i stands for the newly transformed orbitals u_i. This process thus mixes molecular orbitals of different symmetries, by variations of θs. This procedure preserves the orthogonality of the MOs, and leaves the two-electron energy E_2 unchanged. The total energy and total density also remain unchanged. This transformation which maximizes D, the intra-orbital Coulomb repulsion energy, also minimizes the inter-orbital Coulomb repulsion

$$\sum_{i>j} 4(ii|jj),$$

Table 1. Occupied α-spin LMOs for the planar monocyclopolyenes.

Molecule	$N(a)$	LMO number	Energy (a.u)	Main AO components (%)	Bonding assignment		Figure number
$C_3H_3^+$	2	1–3	−1·373	C(48·98) + C′(48·98)	σ(C–C)	(3×)	
		4–6	−1·251	C(57·99) + H(41·93)	σ(C–H)	(3×)	
		7	−1·089	C(33·33) + C′(33·33) + C″(33·33)	π(C–C–C)		1(*a*)
$C_3H_3^-$	4	1	−0·719	C(48·49) + C′(48·49)	σ(C–C)		
		2–3	−0·609	C(56·31) + C′(41·48)	σ(C–C)	(2×)	
		4–5	−0·596	C(45·39) + H(54·39)	σ(C–H)	(2×)	
		6	−0·500	C(47·94) + H(51·92)	σ(C–H)		
		7	−0·219	C(50·00) + C′(50·00)	π(C–C)		2(*a*)
		8	−0·018	C(100·00)	λ(C)		
$C_4H_4^{2+}$	2	1–4	−1·722	C(49·44) + C′(49·44)	σ(C–C)	(4×)	
		5–8	−1·515	C(60·36) + C′(39·44)	σ(C–H)	(4×)	
		9	−1·425	$C_1(25·00) + C_2(25·00) + C_3(25·00) + C_4(25·00)$	π(C–C, C–C)		3(*a*)
C_4H_4(*b*)	4	1,2	−1·103	C(49·41) + C′(49·41)	σ(C–C)	(2×)	
		3,4	−1·041	C(48·98) + C′(48·98)	σ(C–C)	(2×)	
		5–8	−0·890	C(50·11) + H(49·53)	σ(C–H)	(4×)	
		9–10	−0·599	C(50·00) + C′(50·00)	π(C–C)	(2×)	4(*a*)
$C_4H_4^{2-}$	6	1–4	−0·419	C(48·96) + C′(48·96)	σ(C–C)	(4×)	
		5–8	−0·281	C(39·89) + H(59·65)	σ(C–H)	(4×)	
		9	0·125	C(63·35) + C′(32·85)	π(C–C)		5(*a*)
		10	0·128	C(64·79) + C′(30·76)	π(C–C)		5(*b*)
		11	0·172	C(7·39) + C′(74·72) + C″(6·50)	π(C–C–C)		5(*c*)

$C_5H_5^+$	4	1	−1·388	C(49·55) + C′(49·55)	σ(C–C)		
		2, 3	−1·384	C(46·29) + C′(52·79)	σ(C–C)	(2×)	
		4, 5	−1·374	C(47·58) + C′(51·45)	σ(C–C)	(2×)	
		6	−1·198	C(52·82) + H(46·64)	σ(C–H)		
		7, 8	−1·176	C(53·16) + H(45·72)	σ(C–H)	(2×)	
		9, 10	−1·144	C(55·16) + H(44·27)	σ(C–H)	(2×)	
		11	−0·913	C(33·05) + C′(57·10) + C″(8·80)	π(C–C–C)		6(*a*)
		12		C(33·09) + C′(57·08) + C″(8·78)	π(C–C–C)		6(*b*)
$C_5H_5^-$	6	1–5	−0·791	C(49·39) + C′(49·39)	σ(C–C)	(5×)	
		6–10	−0·608	C(45·41) + H(53·98)	σ(C–H)	(5×)	
		11		C(19·32) + C′(59·92) + C″(15·66)	π(C–C–C)		7(*a*)
		12	−0·284	C(54·59) + C′(34·37)	π(C–C)		7(*b*)
		13		C(38·50) + C′(51·86) + C″(6·31)	π(C–C–C)		7(*c*)
C_6H_6	6	1–6	−1·092	C(49·52) + C′(49·52)	σ(C–C)	(6×)	
		7–12	−0·885	C(49·48) + H(49·76)	σ(C–H)	(6×)	
		13–15	−0·625	C(24·10) + C′(49·92) + C″(20·38)	π(C–C–C)	(3×)	8(*a*, *b*, *c*)
$C_6H_6^{2-}$	8	1, 2	−0·559	C(46·36) + C′(52·55)	σ(C–C)	(2×)	
		3, 4	−0·559	C(46·33) + C′(52·58)	σ(C–C)	(2×)	
		5, 6	−0·535	C(49·29) + C′(49·36)	σ(C–C)	(2×)	
		7, 8	−0·409	C(41·21) + H(57·97)	σ(C–H)	(2×)	
		9, 10	−0·358	C(42·39) + H(56·63)	σ(C–H)	(2×)	
		11, 12	−0·358	C(42·41) + H(56·62)	σ(C–H)	(2×)	
		13, 14	0·010	C(23·37) + C′(73·78)	π(C–C)	(2×)	9(*a*)
		15, 16	0·011	C(22·94) + C′(74·13)	π(C–C)	(2×)	9(*b*)
$C_6H_8(c)$	6	1	−1·124	C(49·72) + C′(49·72)	σ(C–C)		
		2, 3	−1·116	C(50·00) + C′(49·45)	σ(C–C)	(2×)	
		4, 5	−1·052	C(49·27) + C′(49·45)	σ(C–C)	(2×)	
		6, 7	−0·896	C(49·27) + H(49·13)	σ(C–H)	(2×)	
		8, 9	−0·883	C(50·56) + H(49·28)	σ(C–H)	(2×)	
		10–11	−0·885	C(50·56) + H(48·78)	σ(C–H)	(2×)	
		12, 13	−0·878	C(50·30) + H(49·15)	σ(C–H)	(2×)	
		14	−0·625	C(47·47) + C′(47·47)	π(C–C)		10(*a*)
		15, 16	−0·604	C(50·05) + C′(47·32)	π(C–C)	(2×)	10(*b*)

Table 1. (*Continued*).

Molecule	N (*a*)	LMO number	Energy (a.u.)	Main AO components (%)	Bonding assignment	Figure number
		1–7	−1·345	C(49·64) + C′(49·64)	σ(C–C) (7×)	
		8–14	−1·122	C(52·23) + H(46·72)	σ(C–H) (7×)	
$C_7H_7^+$	6	15		C(32·85) + C′(40·71) + C″(14·96)	π(C–C–C)	11 (*c*)
		16	−0·901	C(23·28) + C′(42·84) + C″(24·80)	π(C–C–C)	11 (*b*)
		17		C(13·57) + C′(39·97) + C″(34·14) + C‴(6·80)	π(C–C, C C)	11 (*a*)
		1	−0·849	C(50·03) + C′(49·13)	σ(C–C)	
		2	−0·848	C(48·31) + C′(50·84)	σ(C–C)	
		3	−0·847	C(51·40) + C′(47·72)	σ(C–C)	
		4	−0·845	C(47·50) + C′(51·62)	σ(C–C)	
		5	−0·844	C(47·67) + C′(51·42)	σ(C–C)	
		6	−0·843	C(48·22) + C′(50·84)	σ(C–C)	
		7	−0·842	C(50·00) + C′(49·06)	σ(C–C)	
		8	−0·669	C(44·86) + H(54·10)	σ(C–H)	
$C_7H_7^-$	8	9	−0·664	C(45·06) + H(53·88)	σ(C–H)	
		10	−0·656	C(45·42) + H(53·49)	σ(C–H)	
		11	−0·647	C(45·87) + H(53·01)	σ(C–H)	
		12	−0·638	C(46·31) + H(52·53)	σ(C–H)	
		13	−0·630	C(46·66) + H(52·15)	σ(C–H)	
		14	−0·625	C(46·84) + H(51·94)	σ(C–H)	
		15	−0·327	C(43·83) + C′(53·93)	π(C–C)	12 (*a*)
		16	−0·325	C(62·83) + C′(33·50)	π(C–C)	12 (*b*)
		17	−0·323	C(23·57) + C′(69·73) + C″(4·04)	π(C–C–C)	12 (*c*)
		18	−0·321	C(15·04) + C′(73·50) + C″(8·43)	π(C–C–C)	12 (*d*)

		1–8	−1·563	C(49·72) + C(49·72)	σ(C–C)	(8 ×)	
		9–16	−1·328	C(54·36) + H(44·43)	σ(C–H)	(8 ×)	
$C_8H_8^{2+}$	8	17		C(16·07) + C′(35·54) + C″(31·57) + C‴(10·11)	π(C–C / C C)		13 (*a*)
		18	−1·129	C(17·27) + C′(30·62) + C″(36·07) + C‴(9·10)	π(C–C / C C)		13 (*b*)
		19		C(24·87) + C′(37·49) + C″(23·69)	π(C–C–C)		13 (*c*)
		1–8	−1·098	C(49·70) + C(49·61)	σ(C–C)	(8 ×)	
C_8H_8	8	9–12	−0·883	C(48·73) + H(49·99)	σ(C–H)	(4 ×)	
		13–16	−0·882	C(48·78) + H(49·93)	σ(C–H)	(4 ×)	
		17–20	−0·605	C(46·79) + C′(46·75)	π(C–C)	(4 ×)	14 (*a*)
		1–8	−0·632	C(49·58) + C′(49·58)	σ(C–C)	(8 ×)	
		9–16	−0·441	C(43·19) + H(55·46)	σ(C–H)	(8 ×)	
		17	−0·101	C(50·38) + C′(40·09)	π(C–C)		15 (*a*)
$C_8H_8^{2-}$	10	18	−0·100	C(51·85) + C′(38·27)	π(C–C)		15 (*b*)
		19	−0·099	C(27·03) + C′(59·06) + C″(5·59)	π(C–C–C)		15 (*c*)
		20	−0·099	C(25·24) + C′(59·89) + C″(6·51)	π(C–C–C)		15 (*d*)
		21	−0·098	C(15·21) + C′(62·48) + C″(13·77)	π(C–C–C)		15 (*e*)
		1, 2	−1·073	C(49·31) + C′(49·31)	σ(C–C)	(2 ×)	
		3–6	−1·057	C(49·25) + C′(49·78)	σ(C–C)	(4 ×)	
		7, 8	−0·986	C(49·41) + C′(49·41)	σ(C–C)	(2 ×)	
$C_8H_8(d)$	8	9–12	−0·880	C(48·67) + H(49·23)	σ(C–H)	(4 ×)	
		13–16	−0·878	C(48·83) + H(49·76)	σ(C–H)	(4 ×)	
		17, 18	−0·776	C(48·75) + C′(48·75)	σ(C–C)	(2 ×)	
		19, 20	−0·667	C(49·01) + C′(49·01)	σ(C–C)	(2 ×)	
		1	−1·319	C(49·72) + C′(49·72)	σ(C–C)		
		2, 3	−1·318	C(50·74) + C′(48·71)	σ(C–C)	(2 ×)	
		4, 5	−1·318	C(51·26) + C′(48·18)	σ(C–C)	(2 ×)	
		6, 7	−1·316	C(51·04) + C′(48·38)	σ(C–C)	(2 ×)	
		8, 9	−1·315	C(50·22) + C(49·18)	σ(C–C)	(2 ×)	
$C_9H_9^+$	8	10	−1·106	C(50·16) + H(48·30)	σ(C–H)		

Table 1. (*Continued*).

Molecule	N (*a*)	LMO number	Energy (a.u.)	Main AO components (%)	Bonding assignment		Figure number
$C_9H_9^+$	8	11, 12	−1·102	C(50·36) + H(48·30)	σ(C–H)	(2×)	
		13, 14	−1·093	C(50·84) + H(47·77)	σ(C–H)	(2×)	
		15, 16	−1·082	C(51·39) + H(47·17)	σ(C–H)	(2×)	
		17, 18	−1·075	C(51·74) + H(47·77)	σ(C–H)	(2×)	
		19, 20	−0·844	C(38·87) + C′(50·71) + C″(6·22)	π(C–C–C)	(2×)	16 (*a*)
		21, 22	−0·844	C(25·67) + C′(57·76) + C″(14·23)	π(C–C–C)	(2×)	16 (*b*)
$C_9H_9^-$	10	1–9	−0·881	C(49·66) + C′(49·66)	σ(C–C)	(9×)	
		10–18	−0·674	C(46·04) + H(52·48)	σ(C–H)	(9×)	
				C(30·60) + C′(52·42) + C″(8·57)	π(C–C–C)		17 (*a*)
				C(26·14) + C′(54·24) + C″(11·69)	π(C–C–C)		17 (*b*)
		19–23	−0·377	C(45·68) + C′(40·64)	π(C–C)		17 (*c*)
				C(20·48) + C′(55·45) + C″(16·45)	π(C–C–C)		17 (*d*)
				C(36·41) + C′(48·99) + C″(5·22)	π(C–C–C)		17 (*e*)

(*a*) N denotes the number of π electrons.
(*b*) Cyclobutadiene.
(*c*) Hexatriene.
(*d*) Cyclooctatetraene.
Note: figure number denotes the number in figure 4.

and minimizes the exchange energy

$$-\sum_{i>j} 2(ij|ij).$$

The atomic contributions for each of the LMOs are obtained by means of Mulliken population analysis, and the non-diagonal elements F_{ij} of the $\mathbf{F}^{LMO}$ matrix are regarded as the interaction energies between the ith and jth LMOs.

It is interesting to note that these LMOs serve as an important conceptual and quantitative link between chemical intuition and quantum theory for molecules and solids. They are in general intuitively much more visualizable than the CMOs, particularly when they are equivalent MOs on account of the inherent symmetry.

2.2. *Localized molecular orbital of benzene*

Benzene is well known to be an aromatic prototype. The α spin occupied LMO energy levels, orbital compositions, and bonding assignments are listed in table 1 and shown in figure 2. It is obvious that the six CMOs with a_{1g}, e_{1u}, e_{1g}, and b_{2u} symmetry are localized between adjacent carbon atoms with σ-bonding characteristics, in the lowest energy level, and thus correspond obviously to the six σ(C–C) bonds in the valence bond theory. Then the six CMOs with a_{1g}, b_{1u}, e_{1u}, e_{2g} symmetry are also

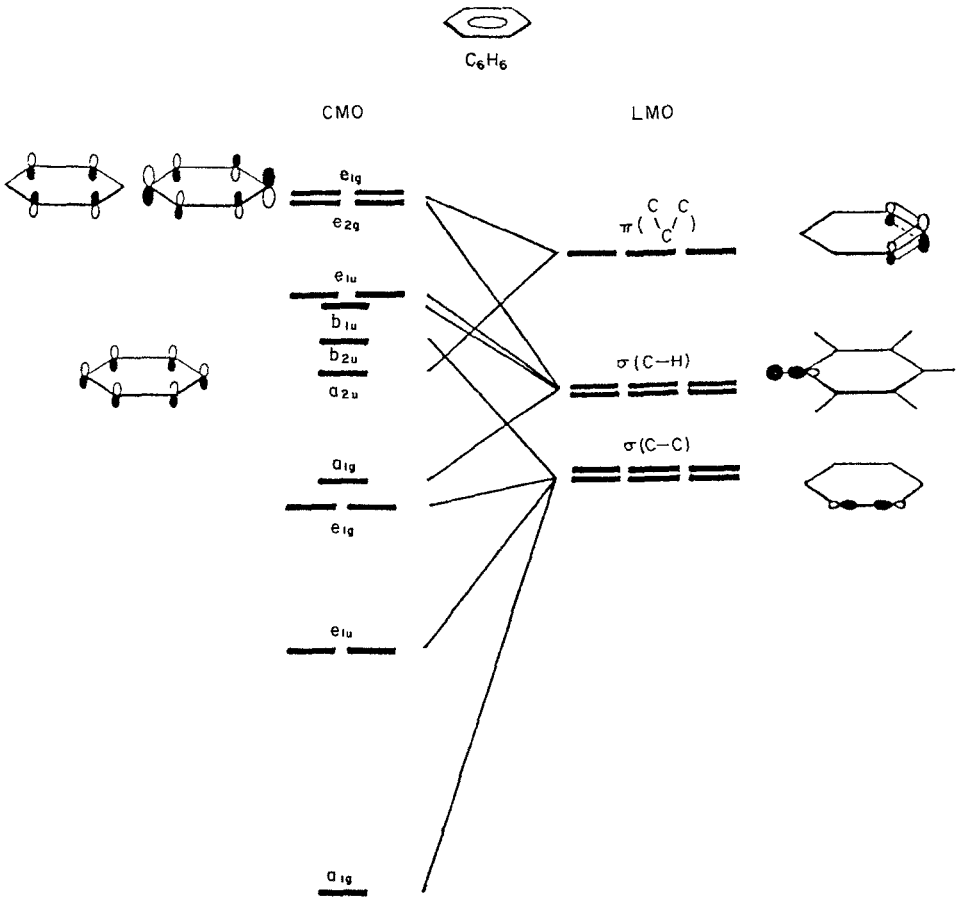

Figure 2. CMOs and LMOs of the benzene molecule.

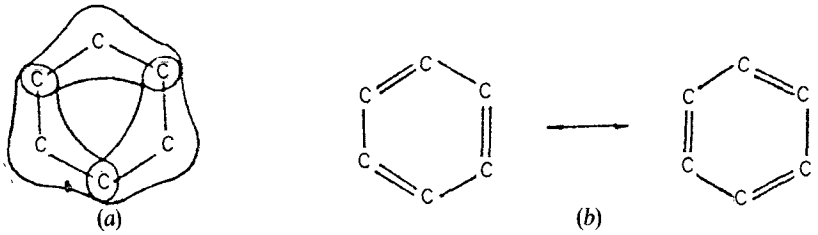

(a) (b)

Figure 3. Molecular structural formula of C_6H_6: (*a*) three-centred two-electron π-bond model; (*b*) two Kekulé structures in dynamic equilibrium.

transformed to two centred LMOs corresponding to the six σ(C–H) bonds. It is interesting that the three π CMOs with a_{2u} and e_{1g} symmetry are localized in space in three adjacent carbon atoms respectively, each of which is formed from the three p_z AOs, perpendicular to the molecular plane, forming an 'island', more or less in the sense of Dewar [19]. These three-centred two-electron π LMOs correspond to a new type of three-centred π bond, different from both the ordinary two-centred σ or π bonds and the three-centred σ bonds in boranes and carboranes. It should be pointed out that the three islands are by no means isolated from each other, since each pair of adjacent 'islands' shares only one p_z AO of the common C atom and thus makes them join up each other, with an interaction energy of −0·116 a.u., constituting a large, completely continuous conjugated π-electron system throughout the whole carbon ring. It is interesting to note that such an LMO description of the molecular structure of C_6H_6 is in a sense quite similar to the pair of Kekulé resonance structures for this aromatic molecule (figure 3). The correctness of this LMO quantum-chemical picture for C_6H_6 will be further attested in the next Section and entirely confirmed by a similar calculation carried out for the hexatriene C_6H_8, which shows clearly only three separate ordinary two-centred π bonds as shown in the next Section. We therefore believe that the cooperative effect among these multi-centred (by this we mean at least three-centred) π bonds are the most significant microscopic features of aromatic compounds.

2.3. *Localized molecular orbitals of planar monocyclopolyenes*

The Hückel Rule predicts that conjugated monocyclic molecules and ions with $(4n+2)$ π electrons are aromatic, whereas those with $4n$ π electrons are not. So far considerable amount of work had been done in connection on this rule. We are interested in comparing bonding characteristics in aromatic against non-aromatic compounds on the basis of our earlier investigation on the LMOs of benzene, for use in our quantum chemical analysis of the problem of quasi-aromaticity in transition metal cluster compounds. The following pairs of molecules or ions are studied herein: $C_3H_3^+$ and $C_3H_3^-$, $C_4H_4^{2+}$ and $C_4H_4^{2-}$ as well as C_4H_4 (cyclobutadiene), $C_5H_5^+$ and $C_5H_5^-$, C_6H_6 and $C_6H_6^{2-}$ along with C_6H_8 (hexatriene), $C_7H_7^+$ and $C_7H_7^-$, $C_8H_8^{2+}$, C_8H_8, C_8H_8 (cyclooctatetraene), and $C_8H_8^{2-}$, $C_9H_9^+$ and $C_9H_9^-$, either found to exist in nature or hypothetical, as well as some reference molecules. For all these eighteen molecules of planar monocyclopolyenes studied, α-spin occupied LMOs are listed in table 1. Figure 4 shows the contour maps of π-type LMOs with three types of π LMOs: 2*a*, 8*a*, and 13*a* in figure 4, corresponding respectively to the two-, three- and four-centred two-electron π bonds. The scheme of chemical bonding in figure 5 gives brief quantum-chemical pictures for the π electrons of the molecules studied.

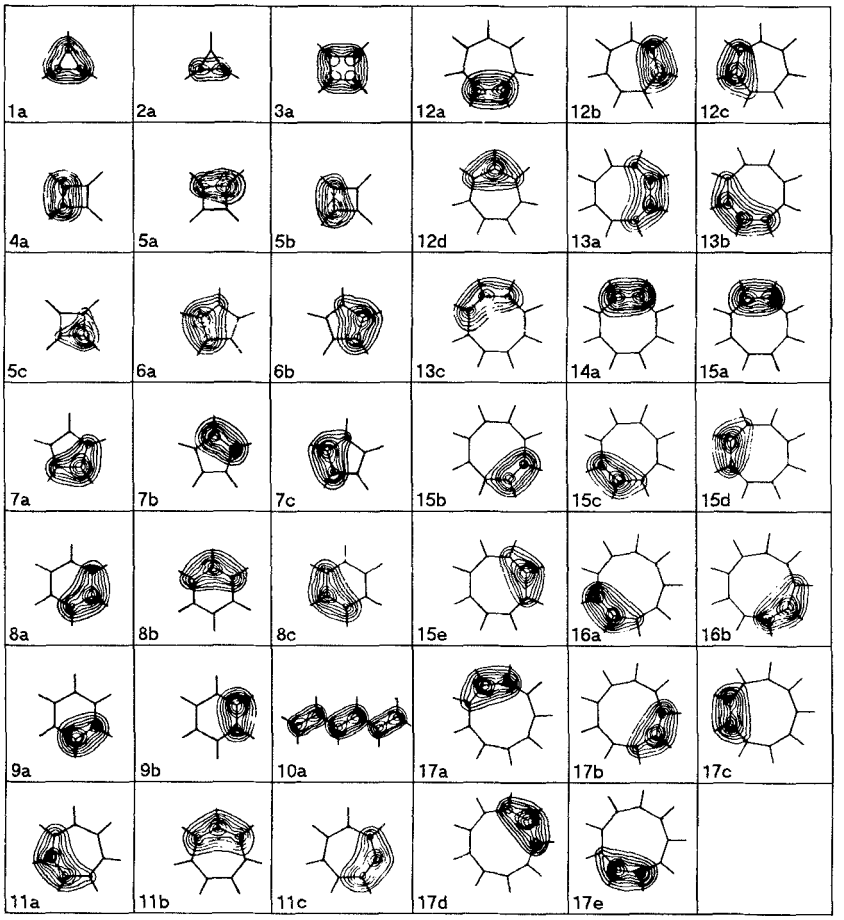

Figure 4. The contour map of LMO wavefunctions for the planar monocyclopolyene hydrocarbons studied, plotted in the section parallel to the molecular plane at height of 0·01 Å. The contour lines (from the innermost to the outmost) correspond respectively to the following values of wavefunction 3, 4, 5, 6, 7, 8, 9, 10 ($\times 10^{-3}$).

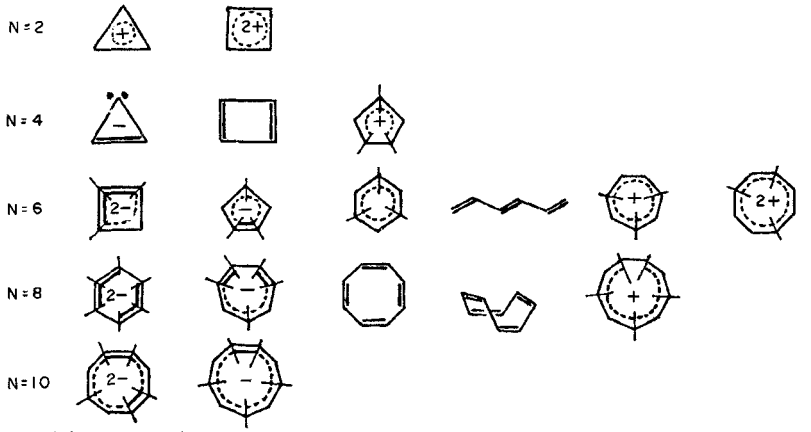

Figure 5. Diagrammatic representation of π bonds for the planar monocyclopolyene hydrocarbons and the reference molecules studied. Two-centred π bond (=), and multicentred π bond (- - - -).

Similar to benzene, there are also some CMOs which can only be transformed into non-classical multi-centred π bonds. Again, they cannot at all be described whatsoever in terms of a single ordinary double bond. This is certainly new within the realm of the ordinary valence bond theory. It is thus understandable that these multi-centred bonds can only be found in molecules which cannot be represented in terms of single valence bond structures, such as $C_3H_3^+$, $C_4H_4^{2-}$, $C_5H_5^+$, $C_5H_5^-$, C_6H_6, $C_7H_7^+$, $C_7H_7^-$, $C_8H_8^{2+}$, $C_8H_8^{2-}$, $C_9H_9^+$, and $C_9H_9^-$. On the contrary, in the molecules with unique valence structures, for example cyclobutadiene C_4H_4, hexatriene C_6H_8, cyclooctatetraene C_8H_8, there exist only isolated two-centred π bonds without any multi-centred π bonds. It appears that the concept of multi-centred bond may be advantageously introduced into the simple valence bond theory for description of 'complex' molecules.

It is obvious that in connection with the delocalizability of π-electron bonding, the non-aromatic reference molecules with unique valence bond structures such as cyclobutadiene, hexatriene and cyclooctatetraene, differ indeed from both the experimentally established aromatic hydrocarbons $C_3H_3^+$, $C_5H_5^-$, C_6H_6, $C_7H_7^+$, $C_8H_8^{2-}$, and $C_9H_9^-$ and the theoretical aromatic systems $C_4H_4^{2-}$, $C_8H_8^{2-}$ with non-unique valence bond structures. It should also be noted that there also exist multi-centred bonds in the anti-aromatic reference molecules $C_5H_5^+$, $C_7H_7^-$, and $C_9H_9^+$. Therefore, a π system with multi-centred bonds cannot be taken as the sole criterion of aromaticity. It is necessary for the aromaticity of monocyclopolyene molecules or ions that the π electrons must form a closed, completely continuous π-conjugated system. On the contrary, in the case of anti-aromatic hydrocarbons, such π-electron systems are usually discontinuous. The scheme in figure 5 clearly shows the bonding characteristics of the π-electron systems for $C_5H_5^+$, $C_7H_7^-$, and $C_9H_9^+$. Hence the existence of a multi-centred π bond only implies the delocalization of π electrons over a region larger than the space limited to two adjacent atoms and covering at least three adjacent atoms. In other words, a closed continuous π bond system, which forms an overall completely continuous conjugated π-electron distribution throughout the carbon ring, gives rise to an additional stability as well as unusual chemical reactivity in the molecule.

It may be interesting to point out that some carbon atoms in the monocyclopolyene molecules studied involve more than four LMOs. Thus in the case of benzene, the carbon atom shared by two adjacent three-centred π bonds involves five LMOs: two σ(C–C) bonds, one σ(C–H) bonds, and two (C–C–C) π bonds, as shown in figure 2. In this case, such a carbon atom appears to have violated the octet rule in the valence bond theory. Lipscomb and others [20, 21] have well discussed this problem, and have proposed that these should be called fractional bonds. Therefore, for the carbon atom shared by two adjacent three-centred two-electron π bonds in the C_6H_6 molecule, the three-centred two-electron π bonds involved are all fractional bonds, and thus there is not at all violation of the octet rule.

2.4. *Localized molecular orbitals for some typical conjugated six-membered rings*

For conjugated six-membered rings, C_6H_6, $C_3N_3H_3$, $B_3N_3H_6$, and $(B_3O_6)^{3-}$ are well known to be aromatic or quasi-aromatic, while $P_3N_3Cl_6$ is a reference molecule experimentally established to be out-of-plane non-aromatic. For convenience of comparison, the LMOs of C_6H_6 is again given herein. The occupied α-spin localized MOs of the five molecules studied are listed in table 2. Figure 6 shows the energy level diagram of the localized MOs for the five molecules studied, with the HOMO taken to be located at the same energy level for these molecules. The contour maps of the LMOs corresponding to the three-centred two-electron π bonds are shown in figure 7.

Table 2. α-Spin occupied LMOs of C_6H_6, $C_3N_3H_3$, $B_3N_3H_6$, $(B_3O_6)^{3-}$, and $P_3N_3Cl_6$.

Molecule	LMO number	Energy (a.u.)	Main AO components (%)	Bonding assignment	
C_6H_6	1–6	−1·092	C(49·5) + C(49·5)	σ(C–C)	(6×)
	7–12	−0·885	C(49·4) + H(49·4)	σ(C–H)	(6×)
	13–15	−0·625	C(24·1) + C′(49·9) + C″(20·4)	π(C–C–C)	(3×)
$C_3N_3H_3$	1–6	−1·145	C(45·3) + N(53·7)	σ(C–N)	(6×)
	7–9	−0·947	C(47·9) + H(51·6)	σ(C–H)	(3×)
	10–12	−0·781	N(98·1)	λ(N)	(3×)
	13–15	−0·673	C(19·4) + N(57·8) + C′(19·4)	π(C–N–C)	(3×)
$B_3N_3H_6$	1–6	−1·080	B(33·9) + N(64·6)	σ(B–N)	(6×)
	7–9	−0·954	N(55·1) + H(43·0)	σ(N–H)	(3×)
	10–12	−0·745	B(42·9) + H(56·6)	σ(B–H)	(3×)
	13–15	−0·648	B(12·5) + N(74·0) + B′(12·5)	π(B–N–B)	(3×)
$(B_3O_6)^{3-}$	1–6	−0·449	O(70·0) + B(38·6)	σ(B–O)	(6×)
	7–9	−0·345	O_t(60·7) + B(39·0)	σ(B–O_t)	(3×)
	10–12	−0·214	O_t(99·9)	λ(O_t)	(3×)
	13–15	−0·156	O(97·3)	λ(O)	(3×)
	16–18	−0·001	B(7·2) + O(84·8) + B′(7·2)	π(B–O–B)	(3×)
	19–21	0·152	B(14·2) + O_t(85·2)	λ′(O_t)	(3×)
	22–24	0·154	O_t(95·7)	λ″(O_t)	(3×)
$P_3N_3Cl_6$	1–6	−1·009	Cl(99·0)	λ(Cl)	(6×)
	7–12	−0·928	P(39·8) + N(51·8)	σ(P–N)	(6×)
	13–15	−0·881	N(83·1)	λ(N)	(3×)
	16–21	−0·835	P(36·6) + Cl(62·7)	σ(P–Cl)	(6×)
	22–24	−0·672	P(17·3) + N(64·6) + P′(17·3)	π(P–N–P)	(3×)
	25–30	−0·623	Cl(90·6)	λ(Cl)	(6×)
	31–36	−0·621	Cl(91·5)	λ(Cl)	(6×)

Subscript '*t*' denotes terminal atom.

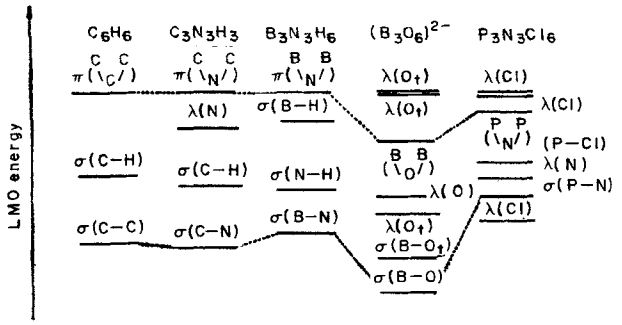

Figure 6. LMO energy level diagram for C_6H_6, $C_3N_3H_3$, $B_3N_3H_6$, $(B_3O_6)^{3-}$, $P_3N_3Cl_6$ with the HOMO assumed to be located at the same energy level.

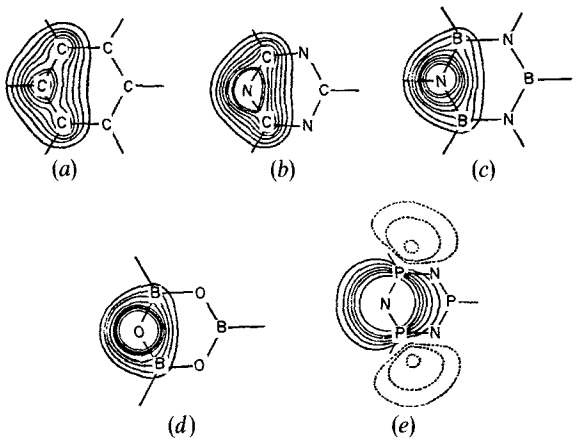

Figure 7. Contour maps for LMOs corresponding to three-centred two-electron π bonds: (*a*) C_6H_6; (*b*) $C_3N_3H_3$; (*c*) $B_3N_3H_6$; (*d*) $(B_3O_6)^{3-}$; (*e*) $P_3N_3Cl_6$.

It is shown that in all these molecules there is an apparent correspondence between the LMOs and the chemical bonds in the ordinary valence bond theory. Furthermore, all the LMOs may be conveniently classified under the three different categories corresponding to the σ, π bonds, and lone-pair electrons, and the LMOs corresponding to the two-centred two-electron bonds and the lone-pair electrons are more than 90% localized except for the 83·1% localization of the lone-pair electrons on the N atom in the P_3N_3 'plane' of $P_3N_3Cl_6$, which will be later discussed in detail. However, the LMOs assigned to the three-centred two-electron π bonds exhibit local delocalization to a good extent.

From the bonding analysis for the molecules studied it is obvious that each three-centred two-electron π bond has particular significance in a conjugated six-membered ring system. It is interesting to note that there exist some differences among different ring systems with the three-centred two-electron π bond. First, from the angle of the constituent atoms, a six-membered ring system with three three-centred π bonds formed from atoms of one kind alone, as in the case of C_6H_6, may start its 'first' atom from an arbitrary atom site around the ring. On the other hand, when the ring system consists of two different kinds of atoms alternately located around the ring, the 'apical' atom of any three-centred π bond must have an electronegativity at least as large as that of the two 'terminal' atoms. Thus it can be seen that in the case of $[C_3N_3]$, $[B_3N_3]$, $[B_3O_3]$, and $[P_3N_3]$ ring cores, the 'apical' atoms can only be N or O atoms respectively, the electronegativities of which are certainly larger than those of C, B and P. Secondly, from the angle of the constituent AOs, there are two different types of three-centred π bonds as discussed above. In the case of (p–p–p)π bonds in C_6H_6, $C_3N_3H_3$, $B_3N_3H_6$, and $(B_3O_6)^{3-}$, they are formed from the three p_z AOs perpendicular to the plane of the 'island'. Since each pair of adjacent three-centred π bonds shares only one p_z AO on the common 'terminal' atom, it is bound to give rise to rather large inter-'island' interaction energies: −0·116, −0·115, −0·095, and −0·077 (in a.u. units) for C_6H_6, $C_3N_3H_3$, $B_3N_3H_6$, and $(B_3O_6)^{3-}$ respectively. Thus this large inter-'island' cooperative effect will help to form a large closed, completely continuous conjugated π-electron system for these six-membered ring systems. On the other hand, the LMO of a (d–p–d)π bond for $P_3N_3Cl_6$ is formed from one p_z AO located on the 'apical' N atom

and one d AO contributed by each of the two adjacent 'terminal' P atoms. It should be noted that in the case of (d–p–d)π bonds, the common 'terminal' P atom shared by the pair of adjoining (d–p–d)π bonds possibly uses two mutually different d AOs to form two adjoining (d–p–d)π bonds. This is the case with $P_3N_3Cl_6$, as shown in figure 7. The two nearly orthogonal d AOs of each 'terminal' P atom will overlap maximally with the unique p_z AO on each of the adjoining 'apical' N atoms along the P–N direction. Hence the inter-'island' interaction energy in this case can only be rather small (−0·022 a.u.), far too small for the formation of a closed and completely continuous conjugated π-electron system. In other words, these 'islands' are really isolated islands in Dewar's sense. Such a situation is possibly only when each common 'terminal' P atom has at least two vacant d AOs. This is the case that Dewar has emphasized in [19]. It should be pointed out that for cyclic phosphonitrilic compounds the in-plane delocalization of the lone-pair electrons on the N atom has been noted in literature [22, 23]. Finally, in so far as the electronic origin of the three-centred π bond is concerned, it has been mentioned that in the case of C_6H_6 and $C_3N_3H_3$, each of the three ring atoms forming the three-centred two-electron π bond contributes one electron from its p_z AO. Again, in the case of $P_3N_3Cl_6$, the 'apical' N atom and the 'terminal' P atoms contribute one electron each from their respective p_z and d AOs, rather similar to the case of C_6H_6 and $C_3N_3H_3$. On the other hand, $B_3N_3H_6$ and $(B_3O_6)^{3-}$ differ from C_6H_6, $C_3N_3H_3$, and $P_3N_3Cl_6$ in the fact that the 'apical' atom (N, O) with a lone pair occupying the unique p_z AO (perpendicular to the plane of the 'island') contributes this pair of electrons to the three-centred π bond, since the 'non-coordinated' p AO in each of the 'terminal' B atoms is a unique vacant orbital, thus not capable of contributing any electron to this π bond. It is interesting to point out that the three 'islands' in the ring system of $B_3N_3H_6$ and $(B_3O_6)^{3-}$ are for the same reason not at all isolated from each other, rather similar to C_6H_6 and $C_3N_3H_3$, but by no means similar to $P_3N_3Cl_6$. Therefore we are confident to say that each of these two ring systems, $B_3N_3H_6$ and $(B_3O_6)^{3-}$, is at least quasi-aromatic. Indeed, figure 7 shows quite clearly that our LMO description of the molecular structure for each of the five conjugated six-membered ring systems is in a sense very similar to a pair of Kekulé resonance valence-bond structures.

3. $M_3(\mu_3\text{–}S)(\mu_2\text{–}S)_3(\mu_2\text{–dtp})(\chi\text{–dtp})_3 \cdot L$ (M = Mo, W)

The discrete trinuclear molybdenum cluster compound $[Mo_3(\mu_3\text{–}S)(\mu_2\text{–}S)_3(\mu_2\text{–dtp})(\chi\text{–dtp})_3(OH_2)]$ (I) is the first example known to exhibit aromaticity in transition metal cluster compounds. In this molecule, there is an equilateral triangle of Mo_3 with Mo–Mo bond distance 2·734, 2·763, and 2·766 Å [12], and a triply bridging or capping S_c atom above the plane of the metal atoms and three edge-bridging S_b atoms below it (figure 1), so as to complete a cluster core $[Mo_3S_4]^{4+}$. In addition, each Mo atom is also chelated by a dtp ($[S_2P(OEt)_2]^{-1}$] ligand, while a fourth dtp ligand spans two Mo atoms, but the third Mo atom leaves one rather loose coordination site to be occupied by a monodentate ligand H_2O with one lone electron pair. Each Mo atom of this cluster compound thus has a formal oxidation state of +4.

3.1. *Experimental evidence*

The first convincing evidence for the benzene-like behaviour of this cluster compound was obtained in the 1987 by Huang and his co-workers [12] from their systematic chemical reactivity studies and crystal structure analyses. Structurally, the six Mo–S_b bonds have an average length of 2·28 Å, which are the shortest in this compound, significantly shorter than the bonds Mo–S_c (2·340 Å) and Mo–S_t (2·566 Å)

(*t* denotes terminal ligand). They lie in between the single bond Mo–S (2·44 Å) and the double bond Mo=S 2·08 Å lengths, resembling the six equivalent C–C bond lengths in the planar benzene ring. This is a clear indication that in addition to a single bond in each of these six Mo–S_b bonds, there should also exist some π delocalization in this puckered six-membered ring $[Mo_3S_3]$ system of alternately located Mo and μ_2–S atoms with two sets of essentially equal bond angles of 96·6° and 74·3° for the bond angles $<(S_b\text{–Mo–}S_b)$ and $<(\text{Mo–}S_b\text{–Mo})$.

The six different types of coordinating ligands in this cluster (namely μ_3–S, μ_2–S, χ–dtp, μ_2–dtp, Mo, $:OH_2$) compound allow it to undergo a great variety of substitution, addition and oxidation reactions. In connection with substitution reactions, this cluster reveals that ligands other than the μ_2–S atoms could be rather readily replaced by other ligands. The loose coordinating ligand H_2O of $Mo_3S_4(dtp)_4H_2O$ can be readily replaced at room temperature by other ligands containing atoms with lone pair electrons such as O, S, N, P:

$$Mo_3S_4(dpt)_4:OH_2 + :L \rightarrow Mo_3S_4(dtp)_4:L,$$

where L = pyridine, oxazole, $PhCH_2SH$, $(CH_2CHCH_2NH)(NH_2)CS$, $PhCH_2CN$, CH_3CH_2CN, Ph_3P.

The chelating dtp and bridging dtp ligands in this cluster compound may also be substituted by appropriate ligands:

$$Mo_3S_4(dtp)_4\cdot H_2O + RCO_2^-, \text{ solvent} \rightarrow Mo_3S_4(\mu_2\text{–}O_2CR)(dtp)_3\cdot(\text{solvent});$$

$$Mo_3S_4(dtp)_4\cdot H_2O + dtc^-, \text{ solvent} \rightarrow Mo_3S_4(dtc)_4\cdot(\text{solvent}).$$

Also, in the presence of some source of S^{2-}, $Mo_3O_cS_3(dtp)_4\cdot H_2O$ can be readily converted to $Mo_3S_4(dtp)_4\ H_2O$ in an acidic solution, while the reverse reaction may take place only when it is refluxed in an acidic medium for a long period of time:

$$Mo_3(\mu_3\text{–S})(\mu_2\text{–S})_3(dtp)_4\cdot H_2O + OH_3^+ \rightarrow Mo_3(\mu_3\text{–O})(\mu_2\text{–S})_3(dtp)_4\cdot H_2O;$$

$$Mo_3(\mu_3\text{–O})(\mu_2\text{–S})_3(dtp)_4\cdot H_2O + H_2S,\ OH_3^+ \rightarrow Mo_3(\mu_3\text{–S})(\mu_2\text{–S})_3(dtp)_4\cdot H_2O.$$

Hence, the reactivity sequence for these ligand substitution reactions is

$$\text{Mo–}O_t(H_2O) > \text{Mo–S}(\mu_2\text{–dtp}) > \text{Mo–S}(\chi\text{–dtp}) > \text{Mo–}(\mu_3\text{–S}) \gg \text{Mo–}(\mu_2\text{–S}),$$

with the $[Mo_3S_3]$ ring remaining essentially intact and invariant, quite similar to the unusually stable $[C_6]$ ring in benzene. A series of substituted compounds of $Mo_3S_4(dtp)_4\cdot H_2O$ are listed in table 3, showing that all the trinuclear molybdenum cluster compounds have the same cluster core structure as the parent cluster $Mo_3S_4(dtp)_4\cdot H_2O$.

For addition reactions of S or *M* atoms (or ions), the puckered $[Mo_3S_3]$ ring appears to enter into reaction as a whole, again quite similar to the addition of H_2 or $[Mo(CO)_3]$ to the benzene ring.

$$Mo_3S_4(dtp)_4\cdot H_2O + H_2S,\ HCl,\ H_2O \rightarrow Mo_3(\mu_3\text{–S})(\mu_2\text{–}S_2)_3(dtp)_3Cl.$$

Though the three bridging S atoms in $Mo_3S_4(dtp)_4\cdot H_2O$ cannot be replaced at all, they can be simultaneously converted to μ_2–S_2 species by addition of S atoms, forming a 'sulphur-rich' compound with the cluster core $[Mo_3S_7]$ leading to increase of the average Mo–S bond length from 2·28 Å of Mo–(μ_2–S) in $Mo_3S_4(dtp)_4H_2O$ to 2·44 Å of Mo–(μ_2–S_2) for the addition product $Mo_3(\mu_3\text{–S})(\mu_2\text{–}S_2)_3(dtp)_3\cdot Cl$. The inverse desulphurization process readily occurs leading the three Mo–(μ_2–S_2) back conversion

Table 3. Important bond lengths in $[Mo_3S_4(dtp)_4(OH_2)]$ and its derivatives (in unit Å).

Compound	Mo–Mo	Mo–μ_3L	(*L*)	Mo–μ_2L	(*L*)	Ref.
$Mo_3S_4(dtp)_4(OH_2)$	2·754	2·346	S	2·283	S	[12]
$Mo_3S_4(dtp)_4[SC(NH_2)(NHC_3H_5)]$	2·755	2·341	S	2·286	S	[12]
$Mo_3S_4(dtp)_4(py)$	2·754	2·339	S	2·282	S	[12]
$Mo_3S_4(dtp)_4(PhCH_2CN)$	2·757	2·341	S	2·284	S	[12]
$Mo_3S_4(dtp)_4(PPh_3)$	2·744	2·333	S	2·288	S	[12]
$Mo_3S_4(dtp)_4(PhCH_2SH)$	2·754	2·337	S	2·282	S	[12]
$Mo_3S_4(dtp)_4$(oxazole)	2·759	2·337	S	2·282	S	[12]
$Mo_3S_4(dtp)_4(CH_3CH_2CN)$	2·754	2·344	S	2·281	S	[12]
$Mo_3(\mu_3\text{–}O)S_3(dtp)_4$(oxazole)	2·638	2·027	S	2·282	S	[12]
$[Mo_3S_4(dtc)_4(py)](py)_2(H_2O)$	2·741	2·343	S	2·289	S	[12]
$Mo_3S_4(dtp)_3$(imidazole)$_3$(dtp)	2·760	2·339	S	2·287	S	[12]
$Mo_3S_4(\mu_2\text{–}O_2CCH_2CH_3)(dtp)_3(py)$	2·731	2·335	S	2·288	S	[12]
$Mo_3S_4(\mu_2\text{–}O_2CH)(dtp)_3(py)$	2·740	2·332	S	2·287	S	[12]
$Mo_3S_4(\mu_2\text{–}O_2CCH_3)(dtp)_3(py)$	2·739	2·334	S	2·293	S	[12]
$[Mo_3S_4(dtp)_3(biphy)](dtp)$	2·751	2·337	S	2·275	S	[12]
$Ba[Mo_3(\mu_3\text{–}S)(\mu_2\text{–}O)_3(Hnta)_3]\cdot 10H_2O$	2·589	2·360	S	1·917	O	[31]
$Ba[Mo_3(\mu_3\text{–}S)(\mu_2\text{–}S)_2(\mu_2\text{–}O)(HN(CH_2CO_2)_2)_3]\cdot 7H_2O$	2·687	2·352	S	2·308 1·943	S O	[32]
$(pyH)_5[Mo_3(\mu_3\text{–}S)(\mu_2\text{–}O)_2(\mu_2\text{–}S)](NCS)_9\cdot 2H_2O$	2·662	2·320	S	2·256 1·945	S O	[30]
$Cs_2[Mo_3O_4(C_2O_4)_3(H_2O)_3]\cdot 4H_2O\cdot 1/2H_2C_2O_4$	2·486	2·019	O	1·921	O	[26]

to the three Mo–(μ_2–S) bonds, and thus resembling to a good extent the three H_2 molecules involved in the hydrogenation and dehydrogenation of benzene. In this case, the C–C bonds of benzene are lengthened from 1·39 Å to 1·54 Å in the hydrogenation products cyclohexane.

Two kinds of metal atoms *M* are involved in addition reactions, one of which involves the main group metals, such as Sb^{3+}, Sn^{2+} having no sufficient valence electrons, unable to form Mo–*M* bonds (for example, the distance 3·8 Å for Mo–Sb). Another case involves the transition metals, such as Mo, W, Fe, Ni, Cu.

$$Mo_3S_4(dtp)_4\cdot H_2O + SbCl_3,\ EtOH \rightarrow Mo_3S_4(dtp)_4(EtOH)\cdot SbCl_3;$$

$$Mo_3S_4(dtp)_4\cdot H_2O + CuI,\ EtOAc,\ DMF \rightarrow Mo_3CuS_4(I)(\mu\text{–}OAc).$$

The simultaneous addition of several metal ion or metal atom to $[Mo_3S_4\cdot 9H_2O]^{4+}$ will be discussed below in detail.

On the other hand, though the crystal of $Mo_3S_4(dtp)_4\cdot H_2O$ is very stable in air, oxidation reaction may occur in solution. Here one of the S_b atoms is oxidized, and at once accompanied by the rupture of two relevant Mo–S_b bonds and the formation of two new Mo=O bonds along with the oxidation of one of the dtp ligands to $[SOP(OEt)_2]^{-1}$, rather similar to the formation of maleic anhydride by catalytic oxidation of benzene (see figure 8).

$$Mo_3S_4(dtp)_4\cdot H_2O + O_2 \rightarrow Mo_3S_3O_2[OSP(OEt)_2](dtp)_3.$$

The W-containing analogue, $W_3(\mu_3\text{–}S)(\mu_2\text{–}S)_3(\mu_2\text{–}dtp)(\chi\text{–}dtp)_3\cdot H_2O$, has been recently reported [24]. This W-containing cluster compound, rather similar to the

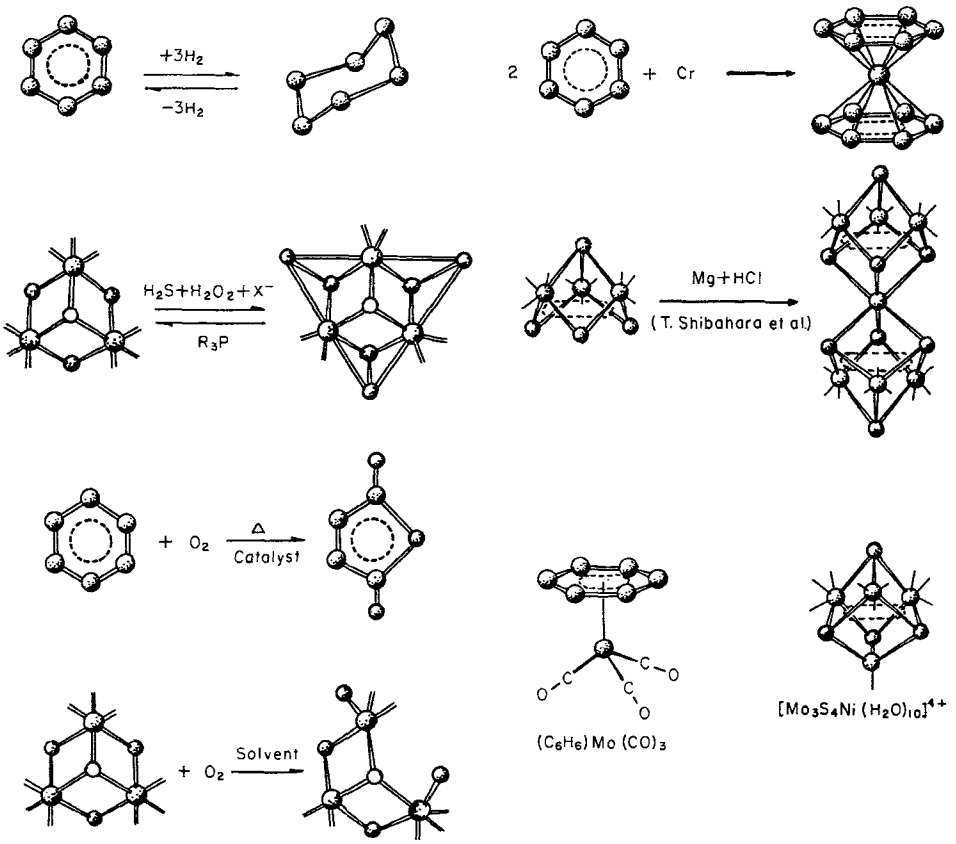

Figure 8. Benzene-like chemical behaviour of $[Mo_3(\mu_3\text{-}S)(\mu_2\text{-}S)_3(\mu_2\text{-}dtp)(\chi\text{-}dtp)_3(OH_2)]$ in addition and oxidation reactions.

Table 4. Important bond lengths in $M_3(\mu_3\text{-}S)(\mu_2\text{-}S)_3(dtp)_3(\mu_2\text{-}OOC_2H_3)C_5H_5N$ (M = Mo, W) (in unit Å) [24].

M	M–M			M–(μ_3–S)	M–(μ_2–S)	M–S(dtp)	M–O	M–N
Mo	2·687	2·762	2·769	2·334	2·293	2·549	2·205	2·385
W	2·672	2·739	2·749	2·343	2·298	2·538	2·174	2·390

Mo-containing one, exhibits also a series of benzene-like behaviours. Table 4 compares the bond lengths in $M_3S_4(dtp)_3(\mu_2\text{-}OOC_2H_3)\cdot C_5H_5N$ (M = Mo, W). The W-containing cluster has the same molecular structure as the Mo-containing cluster, both of which consist of a stable puckered six-membered ring $[M_3(\mu_2\text{-}S)_3]$ with shorter distances of M–(μ_2–S) bond.

In connection with substitution reactions, it is at once evident that for the loose ligand the following reaction occurs rather easily:

$$W_3S_4(dtp)_4:OH_2 + :L \rightarrow W_3S_4(dtp)_4:L + :OH_2,$$

where $L = CH_3CN$, $PhCH_2CN$, D*M*SO, DMF, C_5H_5N, etc.; for the substitution of the bridging dtp ligand

$$W_3S_4(\mu\text{–dtp})(\chi\text{–dtp})_3 : L \xrightarrow{HOOCR} W_3S_4(\chi\text{–dtp})_3(\mu\text{–OOC}R) : L;$$

and for the terminal ligands

$$[W_3S_4(H_2O)_9]^{4+} + 4\text{dtp} \rightarrow W_3S_4(\text{dtp})_4 \cdot H_2O + 8H_2O.$$

A series of trinuclear tungsten cluster compounds with the $[W_3(\mu_3\text{–S})(\mu_2\text{–S})_3]^{4+}$ core as analogues of Mo-containing cluster compounds have been synthesized by substitution reactions involving different ligands, again, keeping the $[W_3S_3]$ ring intact in substitution reactions. So far as an addition reaction is concerned, the following reactions have been reported:

$$W_3S_4(\text{dtp})_4 \cdot H_2O \xrightarrow[HOOCR]{CuI, L} (W_3CuS_4)(I)(\text{dtp})_3(\mu\text{–OOC}R) \cdot L,$$

where $R = CH_3$, C_6H_5, CCl_3; $L = C_5H_5N$, D*M*F, D*M*SO, $PhCH_2CN$, CH_3CN, H_2O. with addition of Cu^+ cation, the three μ_2–S atoms in $W_3S_4(\text{dtp})_4 \cdot H_2O$ are converted to three μ_3–S atoms, forming a cubane-type mixed metal cluster with the $[W_3CuS_4]^{5+}$ core in which the Cu atom completes its 18-electron configuration, similar to the case of $C_6H_6Cr(CO)_3$.

3.2. *Application of the LMO method*

From the angle of ligand substitution reactions, the $[Mo_3S_4]^{4+}$ core of the cluster molecule $Mo_3S_4(\text{dtp})_4 \cdot H_2O$ may be regarded as a rather stable structural sublevel in itself. Of the 19 α-spin occupied LMOs for $[Mo_3S_4]^{4+}$ (see table 5), the 13 lower-energy LMOs obviously correspond to the four lone electron pairs on the four S atoms, the three Mo–S_c σ bonds and the six Mo–S_b σ bonds of the valence bond theory. Besides, just like the case of C_6H_6, there are three three-centred two-electron π bond (figure 9), with each S_b atom contributing one lone pair of electrons and one p_z AO perpendicular the MoS_bMo plane while each of the two adjoining Mo atoms contributes one vacant d AO, thus forming a three-centred two-electron (d–p–d)π bond shaped like Dewar 'islands', although these three 'islands' are not at all isolated from each other. This bonding LMO has the plane MoS_bMo as a nodal plane. On the side farther away from the atom S_c, the electron clouds from the three 'islands' superpose themselves to form a conical cloud distribution on account of their cooperative effect, leading to a chemical active centre of the molecule at the site of the incomplete cubane-type cluster. On the other hand, such an effect does not exhibit itself to any appreciable extent on the other side of the nodal plane, and thus gives rise to three more or less discrete patches of electron cloud concentrated over the three 'islands' (see the MO 'CT' contour graphs in figure 10), forming three other active centres of the cluster compounds. It should be noted that just like the case of C_6H_6, each pair of adjoining 'islands' shares the same d AO of the common Mo atom with a rather large interaction energy of −0·050 a.u. Moreover, on account of the cooperative effect of the adjoining 'island', this non-planar puckered $[Mo_3S_3]$ ring forms a large three-dimensional closed, completely continuous conjugated π-electron system (similar to the $[C_6]$ ring in C_6H_6 to a certain extent), yet with unsymmetrical electron cloud distributions with respect to each of the three MoS_bMo planes (thus quite different from the planar $[C_6]$ ring in C_6H_6). In addition, the remaining three higher-energy LMOs are seen to correspond to three two-centred two-electron σ(Mo–Mo) bonds.

Table 5. α-Spin occupied LMOs of $[Mo_3O_4]^{4+}$, $[Mo_3S_cO_3]^{4+}$, $[Mo_3O_cS_3]^{4+}$, and $[Mo_3S_4]^{4+}$.

Cluster	LMO number	Energy (a.u.)	Main AO components (%)	Bonding assignment	
$[Mo_3O_4]^{4+}$	1–3	−1·940	O_b(98·99)	$\lambda(O_b)$	(3×)
	4	−1·938	O_c(99·30)	$\lambda(O_c)$	
	5–7	−1·639	Mo(20·95)+O_c(74·41)	σ(Mo–O_c)	(3×)
	8–13	−1·617	Mo(28·24)+O_b(66·64)	σ(Mo–O_b)	(6×)
	14–16	−1·487	Mo(8·35)+O_b(82·85)+Mo′(8·35)	π(Mo–O_b–Mo)	(3×)
	17–19	−1·286	Mo(48·21)+Mo′(48·21)	σ(Mo–Mo)	(3×)
$[Mo_3S_cO_3]^{4+}$	1–3	−1·927	O_b(98·95)	$\lambda(O_b)$	(3×)
	4	−1·663	S_c(98·98)	$\lambda(S_c)$	
	5–10	−1·596	Mo(28·57)+O_b(66·67)	σ(Mo–O_b)	(6×)
	11–13	−1·473	Mo(26·50)+S_c(69·07)	σ(Mo–S_c)	(3×)
	14–16	−1·464	Mo(8·41)+O_b(82·72)+Mo(8·41)	π(Mo–O_b–Mo)	(3×)
	17–19	−1·266	Mo(48·12)+Mo(48·12)	σ(Mo–Mo)	(3×)
$[Mo_3O_cS_3]^{4+}$	1	−1·890	O_c(99·00)	$\lambda(O_c)$	
	2–4	−1·609	S_b(98·53)	$\lambda(S_b)$	(3×)
	5–7	−1·557	Mo(22·05)+O_c(72·91)	σ(Mo–O_c)	(3×)
	8–13	−1·415	Mo(34·66)+S_b(61·11)	σ(Mo–S_b)	(6×)
	14–16	−1·299	Mo(10·68)+S_b(77·81)+Mo(10·68)	π(Mo–S_b–Mo)	(3×)
	17–19	−1·222	Mo(47·84)+Mo′(47·84)	σ(Mo–Mo)	(3×)
$[Mo_3S_4]^{4+}$	1	−1·614	S_c(98·50)	$\lambda(S_c)$	
	2–4	−1·593	S_b(98·40)	$\lambda(S_b)$	(3×)
	5–7	−1·415	Mo(26·80)+S_c(67·50)	σ(Mo–S_c)	(3×)
	8–13	−1·393	Mo(34·30)+S_b(61·70)	σ(Mo–S_b)	(6×)
	14–16	−1·278	Mo(10·50)+S_b(78·00)+Mo(10·50)	π(Mo–S_b–Mo)	(3×)
	17–19	−1·204	Mo(48·30)+Mo′(48·30)	σ(Mo–Mo)	(3×)

λ, σ, π denote lone pair of electrons, σ bond, and π bond respectively. Subscripts *b*, *c*, denote bridging and capping atoms respectively.

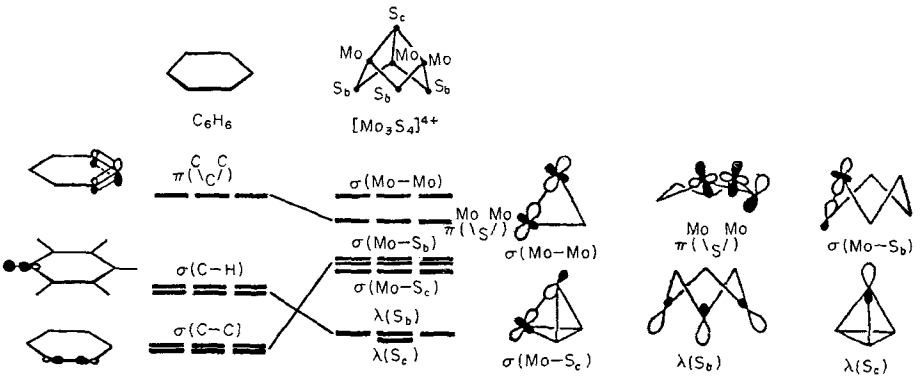

Figure 9. LMOs of C_6H_6 against the $[Mo_3S_4]^{4+}$ cluster core.

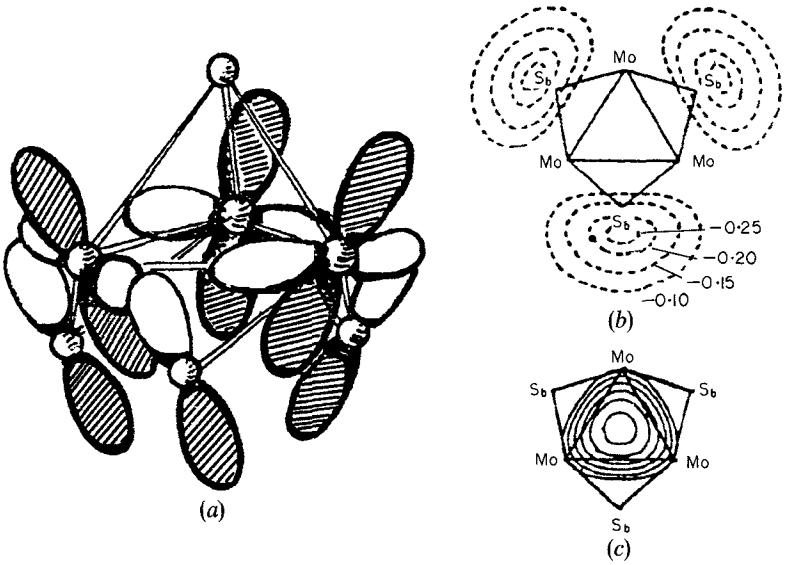

Figure 10. For the $[Mo_3(\mu_3\text{–}S)(\mu_2\text{–}S)_3]^{4+}$ cluster core, (*a*) π LMOs diagrammatic representation; 'CT' view at heights of (*b*) 0·01 Å; (*c*) −1·39 Å (at the $[S_3]$ plane), with lines (from innermost to outmost) corresponding to values of wavefunction: 0·65, 0·60, 0·55, 0·50, 0·45, 0·40. The positions of atoms shown in the diagram are the projection of the cluster core onto the sections.

The LMOs calculated for the overall cluster molecule $Mo_3S_4(dtp)_4 \cdot H_2O$ show that the bonding on the $[Mo_3S_4]$ moiety is quite similar to that in the reduced $[Mo_3S_4]$ cluster core insofar as in either of them there exist three (Mo–S_b–Mo) (d–p–d)π bonds localized in the three adjoining (Mo–S_b–Mo) 'islands' with the same cooperative effect. This leads at once to a clear-cut quantum-chemical interpretation of the benzene-like behaviour of the cluster molecule $Mo_3S_4(dtp)_4 \cdot H_2O$ with regard to its bond length and bond angle structural parameters as well as its ligand substitution, addition and oxidation reactions. (1) the formation of a large three-dimensional closed, completed continuous conjugated π-electron system in the non-planar puckered $[Mo_3S_3]$ cluster ring in the cluster molecule confers upon this ring additional chemical stability, leading to the strengthening of this cluster compound and shortening of the six essentially equivalent M_o–S_b bond lengths; (2) intactness of this $[Mo_3S_3]$ ring in ligand substitution reactions; (3) rupture of this large conjugated π-electron system and the $[Mo_3S_3]$ ring as well, following oxidation of one of the three S_b atoms; (4) two different types (*M*; S) of addition reactions because of the unsymmetrical electron cloud distribution around the puckered $[Mo_3S_3]$ ring (simultaneous addition of three S atoms to form three μ_2–S_2 ligands against addition of only one *M*, such as Mo, W, Fe, Ni, Cu, Sn, Sb). It should be noted that in the addition product $[Mo_3S_7]^{4+}$ there is no longer any three-centred two-electron π bond located on (Mo–S_b–Mo), entirely different from the case of $[Mo_3S_4]^{4+}$ cluster core discussed above. It may serve as more evidence for the nature of quasi-aromaticity in the non-planar puckered $[Mo_3S_3]$ ring of certain $[Mo_3S_4]^{4+}$ clusters. In other words, this quantum-chemical picture of the three-centred two-electron (Mo–S_b–Mo) (d–p–d)π bonds has led us to visualize the $[Mo_3S_3]$ ring as a rather stable structural sublevel in the cluster molecule and to account for its quasi-aromaticity as well. On the other hand, both the (d–p–d) constitution of such a three-centred π bond and the mode of electron labilaty upon bonding are certainly different

from those of C_6H_6. Hence Huang and one of us (Lu) prefer to be more conservative in designating such a benzene-like behaviour as quasi-aromaticity.

In the course of our present work, a study of LMOs of molecules under a different approximation scheme of molecular orbital methods has been completed, allowing us straightforward comparison of the LMOs obtained by the Edmiston–Ruedenberg localized method (I) under the CNDO/2 approximation with those obtained by the Boys localized method (II) following pseudopotential *ab initio* MO calculations [25]. The two methods give qualitatively similar results, thus confirming the quantum-chemical picture of multi-centred bonds with strong interactions for aromatic and quasi-aromatic π-electron systems (see table 10, 11).

4. $[M_3^{IV}(\mu_3\text{–}X)(\mu_2\text{–}Y)_3]^{4+}$ (M = Mo, W; X = O, S; Y = O, S, Se, Te)

The first example of a structurally characterized discrete cluster compound with a $[Mo_3(\mu_3\text{–}X)(\mu_2\text{–}Y)_3]^{4+}$ core isolated by Cotton *et al.* [26] from aqueous solution is $Cs_2[Mo_3O_4(C_2O_4)_3(H_2O)_3]\cdot 4H_2O\cdot 1/2H_2C_2O_4$. X-ray structure analysis shows clearly that the distance Mo–(μ_2–O) (1·921 Å) is significantly shorter than Mo–(μ_3–O) (2·019 Å), and remarkably so than Mo–O(OH_2) (2·15 Å) trans to μ_3–O and Mo–O(ox) (2·091 Å) trans to μ_2–O. On the other hand, Rodgers *et al.* [27] has further reported the rate of exchange of oxygen in $[Mo_3O_4]^{4+}$ with solvent water molecules at 25°C using ^{18}O isotropic tracer techniques. It was found that there were four types of oxygen exchange at very different rates with different half-time as follows: >3 years for μ_2–O atoms, about 5 days for μ_3–O atom, about 1·1 h for H_2O trans to μ_3–O, and about 20 min for H_2O trans to μ_2–O at 0°C. This gives a sufficiently straightforward demonstration that the $[Mo_3(\mu_2\text{–}O)_3]^{6+}$ six-membered puckered ring in the $[Mo_3O_4(C_2O_4)(H_2O)_3]$ cluster compound is in fact kinetically and thermodynamically stable. Huang's experiments [12] also show that when the capping and bridging sulphur atoms in $[Mo_3S_4(H_2O)_9]^{4+}$ are replaced by oxygen atoms, its benzene-like behaviours are by no means significantly changed. The following reactivity sequence in the cluster $[Mo_3(\mu_3\text{–}O)(\mu_2\text{–}O)_3(H_2O)_9]^{4+}$

$$Mo\text{–}O_t(OH_2) > Mo\text{–}(\mu_3\text{–}O) \gg Mo\text{–}(\mu_2\text{–}O),$$

is very much similar to the case of $Mo_3S_4(dtp)_4\cdot H_2O$.

Other prototype clusters $[W_3(\mu_3\text{–}O)(\mu_2\text{–}O)_3(NCS)_9]^{5-}$ and $[W_3(\mu_3\text{–}S)(\mu_2\text{–}S)_3(H_2O)_9]^{4+}$ have also been synthesized and structurally characterized [28, 29]. X-ray structure analysis shows again that both clusters have structures of cluster core similar to those of their Mo analogues, the former with bond distance W–W = 2·534 Å, W–(μ_3–O) = 2·039 Å, W–(μ_2–O) = 1·911 Å and W–N = 2·110 Å, the latter with the correspondingly larger bond distance W–W = 2·724 Å, W–(μ_3–S) = 2·345 Å, W–(μ_2–S) = 2·283 Å owing to the larger size of the S atom, and W–$O_t(OH_2)$ = 2·187 Å. Again, it is seen that the distances W–(μ_2–Y) (Y = O, S) in these two cluster compounds are the shortest bond lengths.

It is noteworthy that numerous discrete triangular trinuclear cluster compounds with $[M_3(\mu_3\text{–}X)(\mu_2\text{–}Y)_3]^{4+}$ cores (M = Mo, W; X, Y = O, S, Se, Te) and various peripheral ligands have been shown to consist of three Mo or W atoms forming essentially equilateral triangles with one capping X atom each above the $[M_3]$ plane and three bridging Y atoms below it, thus making a distorted octahedral coordination environment around each Mo or W atom with M–M bonds [9, 10, 30]. It should be noted that some mixed metal clusters with $[M_{3-n}M'_n(\mu_3\text{–}X)(\mu\text{–}Y)_3]^{4+}$ core (M,

Table 10. Main AO components (%) of occupied π-type LMOs calculated by method I and method II [25].

Compound	Method I	Method II	
		STO–3G	4–31G
C_6H_6	C(20·6) + C(50·0) + C(24·4)	C(24·4) + C(50·5) + C(20·6)	C(24·4) + C(50·5) + C(20·6)
$C_3N_3H_3$	C(19·5) + N(57·5) + C(19·5)	C(21·3) + N(53·5) + C(21·3)	C(19·1) + N(59·3) + C(19·1)
$B_3N_3H_6$	B(12·6) + N(73·4) + B(12·6)	B(9·4) + N(80·7) + B(9·4)	B(7·4) + N(85·3) + B(7·4)
$(B_3O_6)^{3-}$	B(6·5) + O(78·1) + B(6·5)	B(5·8) + O(87·4) + B(5·8)	B(4·5) + O(91·0) + B(4·5)
$[Mo_3S_4]^{4+}$	Mo(10·6) + S(77·4) + Mo(10·6)	Mo(15·4) + S(58·8) + Mo(15·4)	Mo(15·4) + S(58·8) + Mo(15·4)
$[Mo_3O_4]^{4+}$	Mo(8·4) + O(82·4) + Mo(8·4)	Mo(13·2) + O(68·2) + Mo(13·2)	Mo(13·2) + O(68·2) + Mo(13·2)
$P_3N_3Cl_6$	P(17·3) + N(64·6) + P(17·3)	P(12·1) + N(76·6) + P(12·1)	P(12·1) + N(76·6) + P(12·1)

Table 11. Interaction energy F_{ij} and orbital energy E_i for occupied π-type LMOs calculated by method I and II (a.u.) [25].

Molecule	Method I		Method II			
			STO–3G		4–31G	
	F_{ij}	E_i	F_{ij}	E_i	F_{ij}	E_i
C_6H_6	−0·1194	−0·6336	−0·0586	−0·3377	−0·0562	−0·3897
$C_3N_3H_3$	−0·1120	−0·6652	−0·0625	−0·4455	−0·0596	−0·5085
$B_3N_3H_6$	−0·0958	−0·6465	−0·0392	−0·3746	−0·0356	−0·4390
$(B_3O_6)^{3-}$	−0·0693	0·0225	−0·0322	0·2473	−0·0268	−0·0112
$[Mo_3S_4]^{4+}$	−0·0478	−1·2817	−0·0276	−1·2300	−0·0276	−1·2300
$[Mo_3O_4]^{4+}$	−0·0455	−1·4855	−0·0206	−1·4760	−0·0206	−1·4760
$P_3N_3Cl_6$	−0·0224	−0·6720	−0·0088	−0·7093	−0·0088	−0·7083

M'=Mo, W; X, Y=O, S; n=0, 1, 2, 3) and mixed oxo/sulphido species of Mo/W clusters $[M_3O_nS_{4-n}]^{4+}$ (M=Mo, W) shown in figure 11 have also been reported [10, 31–34] to have isostructures as $[Mo_3(\mu_3\text{–}S)(\mu_2\text{–}S)_3]^{4+}$, this constituting the most important structural type of discrete triangular trinuclear cluster compounds with M–M bonds.

The localized MOs of the kind of cluster compounds with $[M_3^{IV}(\mu_3\text{–}X)(\mu_2\text{–}Y)_3]^{4+}$ cores reveal some common bonding feature resembling the prototype cluster compound $[Mo_3S_4(dtp)_4 \cdot H_2O]$. The relative energy levels, main atomic contributions and bonding assignments of LMOs for the cluster core $[Mo_3O_4]^{4+}$, $[Mo_3S_cO_3]^{4+}$, $[Mo_3O_cS_3]^{4+}$ and $[Mo_3S_4]^{4+}$ of $Cs_2[Mo_3O_4(C_2O_4)_3(H_2O)_3] \cdot 4H_2O \cdot 1/2H_2C_2O_4$ [26], $Ba[Mo_3S_cO_3(Hnta)_3] \cdot 10H_2O$ [31], $[Mo_3O_cS_3(dtp)_4] \cdot C_3H_3N_2$ [34], $[Mo_3S_4(\mu_2\text{–}dtp)(\chi\text{–}dtp)_3H_2O]$ [35] compounds, respectively, are listed in table 5, figure 12 shows the energy level diagrams of the LMOs for these cluster cores. These four cluster cores have different bridging and capping atoms, although they have quite similar electronic structures in the core frameworks. Of the 19 occupied LMOs, the LMOs for the four lower levels correspond to the four lone pairs of electrons on the bridging and capping atoms. The LMOs of the next nine higher levels correspond obviously to the three σ(Mo–X) and the six σ(Mo–Y). It is important that for all these cores there exist three three-centred two-electron (Mo–Y–Mo) π bonds, as described in the previous Section, with each bridging Y atom contributing one pair of electrons from the lone pair occupying the p_z AO perpendicular to the Mo–Y–Mo plane and each of the two Mo atoms contributing its unique vacant 4d AO, thus forming a (d–p–d) π bond (figure 9). It is seen that the delocalization of the lone pair electrons of the bridging atom onto the two adjoining Mo atoms depends mainly on the size and electronegativity of the bridging atom itself. The populations of the bridging atoms in table 6 show that the degree of delocalization for a bridging S atom is larger than that for a bridging O atom due to the larger atomic volume and smaller electronegativity of the S atom. For the next three highest levels, the LMOs correspond obviously to the three two-centred two-electron (Mo–Mo) σ bonds.

Meanwhile, figure 12 shows clearly how the energy levels of these cluster cores change with the different bridging and capping atoms. In general, the LMO energy

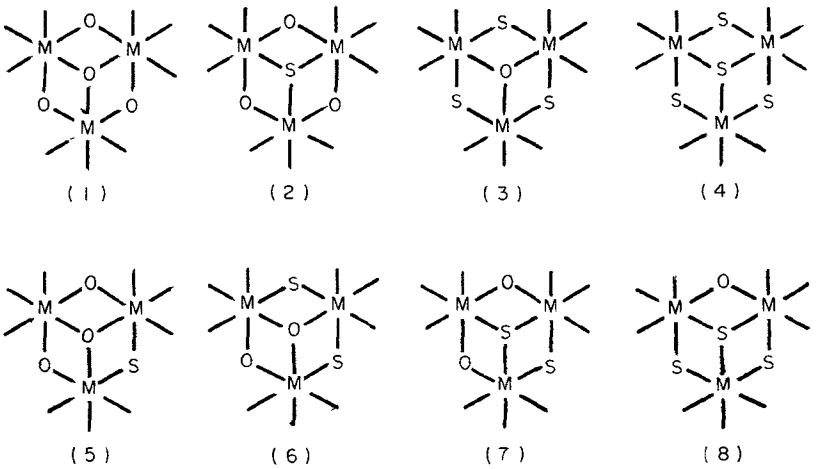

Figure 11. $[M_3O_nS_{4-n}]^{4+}$ (M=Mo, W; n=0, 1, 2, 3, 4).

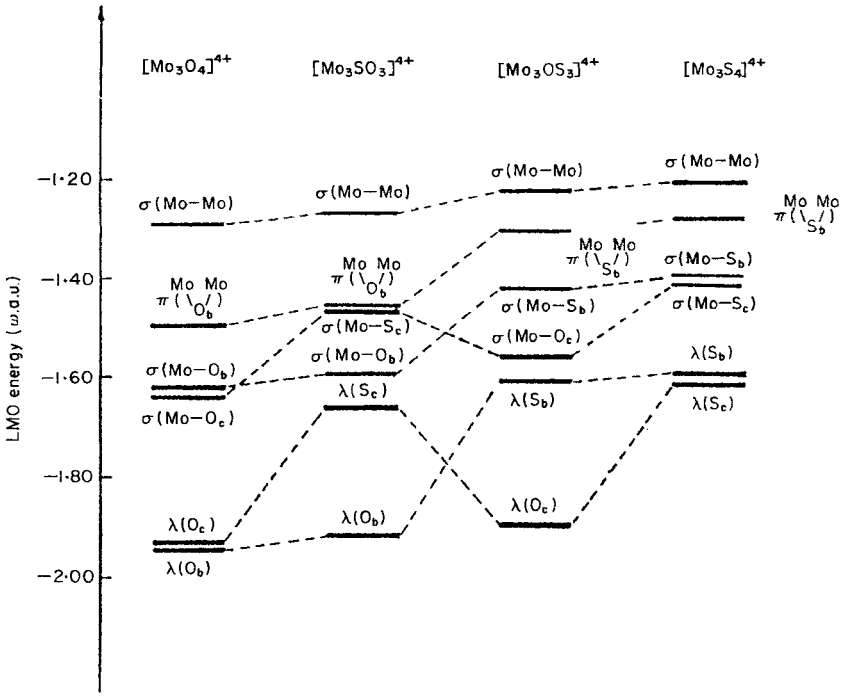

Figure 12. LMO energy levels of $[Mo_3O_4]^{4+}$, $[Mo_3S_cO_3]^{4+}$, $[Mo_3O_cS_3]^{4+}$, $[Mo_3S_4]^{4+}$ (subscripts *b*, *c* denote bridging and capping atoms respectively).

Table 6. Bond lengths and Mulliken bond orders in $[Mo_3O_4]^{4+}$, $[Mo_3S_cO_3]^{4+}$, $[MoO_cS_3]^{4+}$, and $[Mo_3S_4]^{4+}$.

	Atom	$[Mo_3O_4]^{4+}$	$[Mo_3S_cO_3]^{4+}$	$[Mo_3O_cS_3]^{4+}$	$[Mo_3S_4]^{4+}$
Bond length (Å)	Mo–Mo	2·486	2·589	2·638	2·754
	Mo–(μ_3–*X*)	2·019	2·360	2·027	2·346
	Mo–(μ_2–*Y*)	1·921	1·917	2·282	2·283
Mulliken bond order	Mo–Mo	0·324	0·321	0·319	0·302
	Mo–(μ_3–*X*)	0·324	0·435	0·322	0·442
	Mo–(μ_2–*Y*)	0·447	0·449	0·573	0·565

levels for these four cluster cores are raised to some extent as the number of S atoms is increased. In particular, the LMO energy for the σ(Mo–Mo) bonds are only rather inappreciably raised as the bridging O atoms are replaced by the S atoms. On the other hand, the increasing trends for the LMO energies corresponding to the (Mo–*Y*–Mo) π bonds and the σ(Mo–*Y*) bonds are much more apparent, arising essentially for the difference in electronegativity between the valence orbitals of the constituent O and S atoms. The Mulliken bond order, in general, decreases as the bond length increases. However, as shown in table 6, for the Mo–*Y* atom pairs in $[Mo_3O_4]^{4+}$, $[Mo_3S_cO_3]^{4+}$, $[Mo_3O_cS_3]^{4+}$ and $[Mo_3S_4]^{4+}$, the Mulliken bond orders are 0·447,

0·449, 0·573, and 0·565 (in unit e), respectively, while their bond lengths are 1·921, 1·917, 2·282, and 2·283 (in unit Å) in the same order. It may be seen that though the bond lengths of Mo–(μ_2–S) in $[Mo_3O_cS_3]^{4+}$ and $[Mo_3S_4]^{4+}$ are quite a bit larger than those of Mo–(μ_2–O) in $[Mo_3O_4]^{4+}$ and $[Mo_3S_cO_3]^{4+}$, the Mulliken bond orders of Mo–(μ_2–S) are unusually large compared to those of Mo–(μ_2–O). This change in the Mulliken bond orders following the replacement of the bridging O atoms arise indeed from the large delocalization of the lone pair electrons of the bridging S atoms into the vacant 4d AO in each of the two adjoining Mo atoms, resulting in stronger bonding in the (Mo–S_b–Mo) π bonds relative to the (Mo–O_b–Mo) π bonds.

Even though the cluster cores, $[Mo_3O_4]^{4+}$, $[Mo_3S_cO_3]^{4+}$, $[Mo_3O_cS_3]^{4+}$ and $[Mo_3S_4]^{4+}$, all have identical bonding schemes, different bridging atoms make these cluster cores exhibit, more or less, different degrees of quasi-aromaticity. The large delocalizability of the lone pair-electrons in a bridging S atom give rise to a greater stability of the local delocalized (Mo–S_b–Mo) π bond; but on the other hand, it enhances inter-LMO interaction for the three (Mo–S_b–Mo) π bonds. In table 7, the inter-bond interaction energy for the (Mo–*Y*–Mo) π bonds, and the atomic population for the bridging *Y* atom and each of the two adjoining Mo atoms are also listed. Both the interaction energy and the depopulation of the bridging atom show consistently that the three π bonds with bridging S atoms form a more stabilized π-conjugated system around the $[Mo_3S_3]$ ring than in the case of bridging O atoms. Furthermore, the more labile π electrons around the $[Mo_3S_3]$ ring give rise to a larger diamagnetic susceptibility than in the $[Mo_3O_3]$ ring. This conclusion is in good agreement with Shibahara's experimental measurements [36] made for $Ba[Mo_3SO_3(Hnta)_3]\cdot 10H_2O$ and $Ca_{1.5}[Mo_3S_4(Hnta)_2(nta)]\cdot 12H_2O$. It is quite apparent that the size and electronegativity of the bridging atoms, which play a more decisive role in the delocalizability of the lone pair π electrons in the bridging atom, enable the $[Mo_3Y_3]$ ring (*Y*=O, S) to exhibit different degrees of quasi-aromaticity in the cluster compounds containing the cores $[Mo_3(\mu_3\text{–}X)(\mu\text{–}Y)_3]^{4+}$ (*X*, *Y*=O, S).

The LMOs analysis for $[Mo_3S_4(CN)_9]^{5-}$ in $K_5[Mo_3S_4(CN)_9]$, and $[Mo_3S_4(H_2O)_9]^{4+}$ in $[Mo_3S_4(H_2O)_9](CH_3C_6H_4SO_3)_4$ as well as the latter cluster core $[Mo_3S_4]^{4+}$ can account, at least qualitatively, for the effect of terminal ligands on the quasi-aromaticity of the puckered six-membered $[Mo_3S_3]$ ring. It is well known that the anion CN^- is a strong-field ligand, whereas the H_2O molecule is a intermediate-field ligand. The Mo–CN Mulliken bond order (0·69) in the former is about twice as great as Mo–OH_2 (0·36) in the latter. The interaction between the Mo atoms and the terminal ligands causes delocalization of the lone pair electron from the terminal ligands to the Mo atoms, leading reduction of these Mo atoms. The net charges on the Mo atoms in $[Mo_3S_4]^{4+}$, $[Mo_3S_4(H_2O)_9]^{4+}$, and $[Mo_3S_4(CN)_9]^{5-}$

Table 7. Inter-(d–p–d) π-bond interaction energy and atomic population of the LMOs corresponding to these π-bonds in $[Mo_3O_4]^{4+}$, $[Mo_3S_cO_3]^{4+}$, $[MoO_cS_3]^{4+}$, and $[Mo_3S_4]^{4+}$.

Cluster core	$[Mo_3O_4]^{4+}$	$[Mo_3S_cO_3]^{4+}$	$[Mo_3O_cS_3]^{4+}$	$[Mo_3S_4]^{4+}$
Interaction energy (a.u.)	0·045	0·045	0·048	0·050
Mo (%)	8·35	8·41	10·68	10·50
(μ_2–*Y*) (%)	82·85	82·72	77·81	78·00

respectively with 0·885 e, 0·377 e, and 0·052 e show that in the case of the strong-field ligand, the Mo atoms are reduced to lower oxidation states, in which for the Mo atoms the ability to accept the lone pair electrons from the bridging S atoms, forming the three-centred two-electron (Mo–S_b–Mo) π bonds, is less than in higher oxidation states. This results in less degree of delocalization of the lone pair electrons on the bridging S atoms in $[Mo_3S_4(CN)_9]^{5-}$ than that in the $[Mo_3S_4(H_2O)_9]^{4+}$ (see table 8). It is obvious that the quasi-aromaticity of the puckered $[Mo_3S_3]$ ring decreases as the interaction between the cluster core $[Mo_3S_4]^{4+}$ and terminal ligands increases.

It is well known that W and Mo are the elements of the same group in the periodic table and have much similar atomic radii, ionization energies, and electronegativities.

Table 8. α-Spin occupied LMOs of $[Mo_3O_4]^{4+}$, $[Mo_3S_4(H_2O)_9]^{4+}$, and $[Mo_3S_4(CN)_9]^{5-}$.

Cluster	LMO number	Energy (a.u.)	Main AO components (%)	Bonding assignment	
$[Mo_3S_4]^{4+}$	1	−1·604	S_c(95·79)	$\lambda(S_c)$	
	2–4	−1·587	S_b(96·65)	$\lambda(S_b)$	(3×)
	5–7	−1·527	Mo(28·45)+S_c(62·65)	σ(Mo–S_c)	(3×)
	8–13	−1·493	Mo(34·16)+S_b(59·84)	σ(Mo–S_b)	(6×)
	14–16	−1·309	Mo(16·74)+S_b(65·65)+Mo′(16·74)	π(Mo–S_b–Mo)	(3×)
	17–19	−1·232	Mo(48·63)+Mo′(48·63)	σ(Mo–Mo)	(3×)
$[Mo_3S_4(H_2O)_9]^{4+}$	1–6	−1·632	Mo(13·17)+O(86·50)	σ(Mo–O)	(6×)
	7–18	−1·614	O(63·23)+H(36·40)	σ(O–H)	(12×)
	19–21	−1·602	Mo(14·54)+O(85·14)	σ(Mo–O)	(3×)
	22–27	−1·595	O(64·70)+H(34·97)	σ(O–H)	(6×)
	28	−1·338	S_c(97·88)	$\lambda(S_c)$	
	29–31	−1·292	S_b(98·21)	$\lambda(S_b)$	(3×)
	32–34	−1·271	Mo(26·62)+S_c(66·83)	σ(Mo–S_c)	(3×)
	35–40	−1·253	O_t(98·71)	$\lambda(O_t)$	(6×)
	41–43	−1·231	O_t(99·23)	$\lambda(O_t)$	(3×)
	44–49	−1·221	Mo(34·18)+S_b(60·73)	σ(Mo–S_b)	(6×)
	50–52	−1·034	Mo(10·76)+S_b(77·86)+Mo′(10·76)	π(Mo–S_b–Mo)	(3×)
	53–55	−0·937	Mo(48·78)+Mo′(48·78)	σ(Mo–Mo)	(3×)
$[Mo_3S_4(CN)_9]^{5-}$	1–3	−0·584	C(46·45)+N(53·24)	σ(C–N)	(3×)
	4–9	−0·578	C(46·38)+N(53·30)	σ(C–N)	(6×)
	10–12	−0·164	N(99·77)	λ(N)	(3×)
	13–18	−0·158	N(99·78)	λ(N)	(6×)
	19–21	−0·101	Mo(28·43)+C(70·30)	σ(Mo–C)	(3×)
	22–27	−0·096	Mo(28·56)+C(70·21)	σ(Mo–C)	(6×)
	28	−0·093	S_c(99·03)	$\lambda(S_c)$	
	29–31	−0·066	S_b(99·24)	$\lambda(S_b)$	(3×)
	32–34	−0·028	Mo(25·74)+S_c(67·55)	σ(Mo–S_c)	(3×)
	35–40	−0·014	C(40·73)+N(58·93)	σ(C–N)	(6×)
	41–52	−0·008	C(42·32)+N(56·89)	σ(C–N)	(12×)
	53–58	−0·006	Mo(29·20)+S_b(65·68)	σ(Mo–S_b)	(6×)
	59–61	0·176	Mo(6·54)+S_b(86·13)+Mo′(6·54)	π(Mo–S_b–Mo)	(3×)
	62–64	0·329	Mo(47·18)+Mo′(47·18)	σ(Mo–Mo)	(3×)

(1) λ, σ, π denote lone pair of electrons, σ bond, and π bond respectively. Subscripts *b*, *c*, *t* denote bridging, capping and terminal atoms respectively.

(2) The calculation parameters of the Mo atom is same as those of previous calculations, but taken orbital exponent ζ(p) = ζ(s).

Table 9. Addition products of $[Mo_3S_4]^{4+}$ with metal atom or ion M^{q+} (in Å).

Compound	Mo–Mo	Mo–M	Mo–S_c(a)	Mo–S_b(a)	M–S_b(a)	Mo–L(b)	Ref.
$[Mo_3FeS_4(NH_3)_9(H_2O)]^{4+}$	2·794	2·683	2·36	2·36	2·249	2·29	[37(*a*)]
$[Mo_3NiS_4(H_2O)_{10}]^{4+}$	2·755	2·640	2·349	2·333	2·205	2·202	[37(*g*)]
$[Mo_3NiS_4(Hnta)(nta)_2Cl]^{5+}$	2·775	2·668	2·348	2·342	2·215	N:2·317 O:2·142	[37(*g*)]
$[Mo_3CuS_4(dtp)_3(CH_3COO)(H_2O)]$	2·741	2·856	2·333	2·330	2·290	2·527(*c*)	[38]
$[Mo_3SbS_4(dtp)_4 \cdot Cl_3(EtOH)]$	2·735	3·822	2·337	2·308	2·775	2·560(*d*)	[39]
$[(H_2O)_9Mo_3S_4SnS_4Mo_3(H_2O)_9]^{8+}$	2·689	3·712	2·337	2·342	2·627	2·177	[37(*f*)]
$[(H_2O)_9Mo_3S_4MoS_4Mo_3(H_2O)_9]^{8+}$	2·770	3·046	2·350	2·325	2·452	2·18	[37(*c*)]
$[(H_2O)_9Mo_3S_4CoCoS_4Mo_3(H_2O)_9]^{8+}$	2·744(*e*)	2·643	2·343	2·308	2·105	2·200	[37(*h*)]
$[(H_2O)_9Mo_3S_4CuCuS_4Mo_3(H_2O)_9]^{8+}$	2·730(*f*)	2·886	2·329	2·347	2·341	2·17	[37(*e*)]

(*a*) S_b, S_c denote the bridging and capping S atoms in the parent cluster core $[Mo_3S_4]^{4+}$.

(*b*) L denotes the terminal ligand.

(*c*) Mo–S_t(dtp).

(*d*) There are three terminal and one bridging dtp ligands in the cluster compound. Mo–L denotes the distance between Mo atom and the S atom of the terminal ligand.

(*e*) Co–Co = 2·498 Å.

(*f*) Cu–Cu = 2·424 Å.

For the series of $[Mo_3^{IV}O_nS_{4-n}]^{4+}$ and $[W_3^{IV}O_nS_{4-n}]^{4+}$ ($n=0, 1, 2, 3, 4$), their electron structures and bonding pictures resemble each other. There are also the three-centred two-electron (W–S_b–W) π bonds in the cluster core $[W_3^{IV}O_nS_{4-n}]^{4+}$, forming a closed and completely continuous π-conjugated system around the puckered $[W_3Y_3]$ ($Y=$O, S) ring. This interprets well the nature of quasi-aromaticity of the cluster compounds with the core $[W_3^{IV}(\mu_3\text{–}X)(\mu_2\text{–}Y)_3]^{4+}$ (X, $Y=$O, S).

5. $[Mo_3S_4]^{4+}$ cluster ion as a quasi-aromatic ligand

A series of reactions of the S-bridged nido cubane-type $[Mo_3S_4]^{4+}$ cluster ion with a metal atom M or metal cation M^{q+} to give a cubane-type $[Mo_3S_4 \cdot ML_n]^{(4+q)+}$ (M = Mo, W, Fe, Ni, Cu, Sn, Sb; L = ligand), or a sandwich-type $[Mo_3S_4 \cdot M \cdot S_4Mo_3]^{8+}$ (M = Mo, Sn, Hg) and doubly bridged double-cubane-type $[Mo_3S_4 \cdot MM \cdot S_4Mo_3]^{8+}$ (M = Cu, Co) cluster compounds have been recently reported [37–43] (see table 9). These reactions may be formally regarded as the following 'building-block' reactions for rational syntheses of sandwich and half-sandwich mixed metal complexes:

$$[3]+[1]\rightarrow[4], \tag{1}$$

$$[3]+[1]+[3]\rightarrow[7], \tag{2}$$

$$[3]+[1]+[1]+[3]\rightarrow[8], \tag{3}$$

where [3] and [1] denote $[Mo_3S_4]^{4+}$ and M (or M^{q+}) respectively. It is interesting that the reactions (1) and (2) are rather similar to the preparations of the π-bis-arene–metal and arene–metal–carbonyl complexes. Thus structurally these products may also be regarded as sandwich and half-sandwich metal complexes, i.e., quasi-arene–metal complexes with the $[Mo_3S_4]^{4+}$ cluster ion looked upon as a quasi-arene type ligand.

Upon further comparison of the LMOs for the prototype arene–metal sandwich complex $(C_6H_6)_2Cr$ and half-sandwich complex $C_6H_6Cr(CO)_3$ with the sandwich-type $[Mo_3S_4 \cdot M \cdot S_4Mo_3]^{8+}$ and half-sandwich-type $[Mo_3S_4 \cdot ML_n]^{(4+q)+}$ complexes, it is found that there are two types of chemical bonds between the metal M and the ligands L, one of which behaves as an $L(\pi)\rightarrow M$ bond, in which the vacant hybridized AOs of the 'intruder' metal atom (either the six d^2sp^3 octahedral AOs or the four sp^3 tetrahedral AOs) are oriented so as to point toward the octahedral or tetrahedral vertices, and the electrons of the three-centred two-electron π bonds in the arene ligand or quasi-aromatic ligand $[Mo_3S_4]^{4+}$ are donated to these vacant hybridized AOs with appropriate symmetry in the bonding combination. In the other type of M–L bond, the lone electron pair, localized essentially in the d AOs of the 'intruder' metal atom, are backward donated to these ligands to some extent, forming $M(\lambda)\rightarrow L$ bond.

For $(C_6H_6)_2Cr$, the six vacant d^2sp^3 hybridized AOs of the central Cr atom orient themselves respectively towards the centres of electron density of each of the six occupied three-centred two-electron π bonds in the two benzene ligands to form six arene→Cr bonds. On the other hand, the two occupied d type AOs (d_{xy}, $d_{x^2-y^2}$) of the Cr atom interact with the vacant π*-orbital set of the two benzene ligand molecules to back-donate electrons from the metal atom to the benzene ligands, forming an $M\rightarrow$arene type of bonding (see figure 13). In the case of $C_6H_6Cr(CO)_3$, the six vacant hybridized d^2sp^3 AOs of the Cr atom accept the six pairs of electrons from the three-centred two-electron π bonds in the benzene ligand and the three carbonyl ligands. It is interesting to note that there are $Cr\rightarrow C_6H_6$ back-donation bonds in $(C_6H_6)_2Cr$, while there are only $Cr\rightarrow CO$ in $C_6H_6Cr(CO)_3$ (see figure 14).

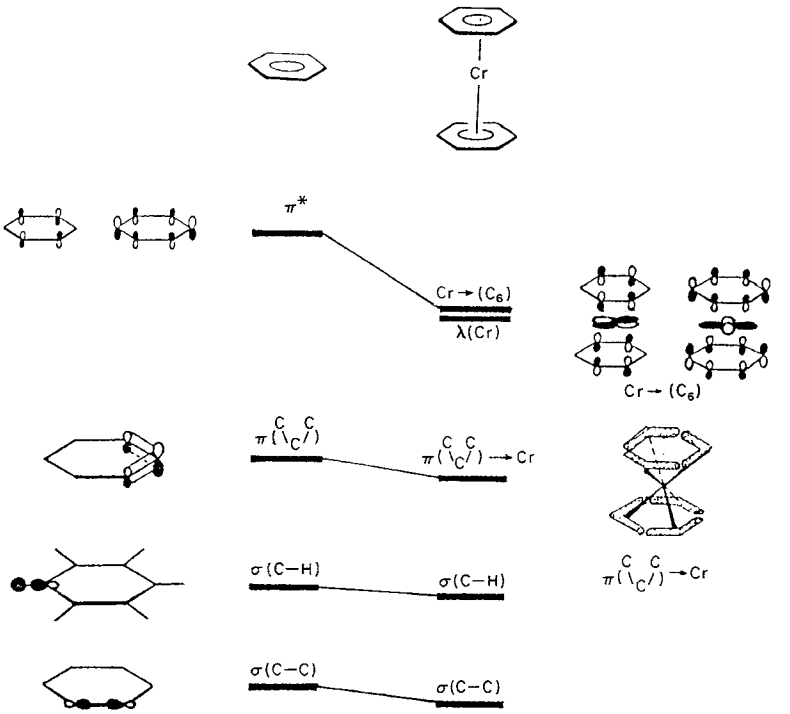

Figure 13. Energy levels and diagrammatic representation of the LMOs for $(C_6H_6)_2Cr$.

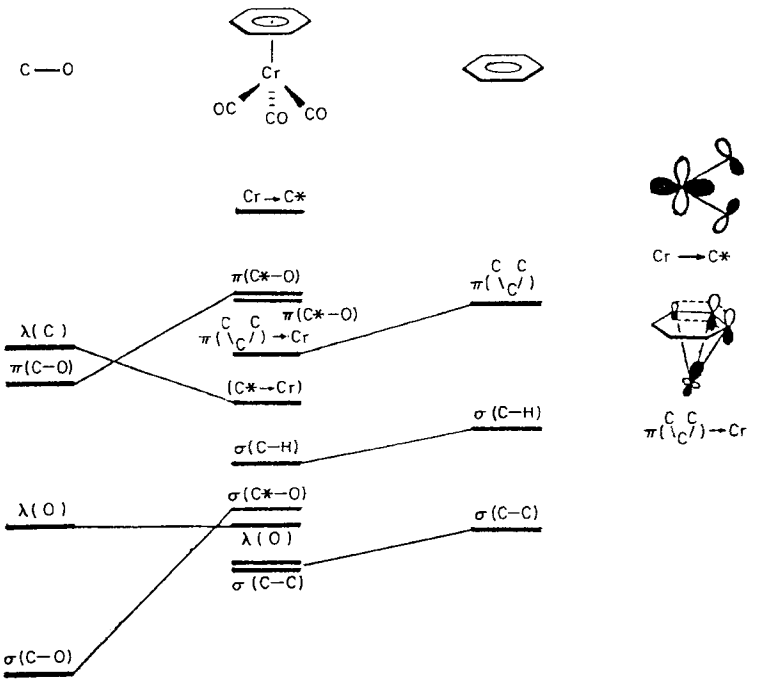

Figure 14. Energy levels and diagrammatic representation of the LMOs for $C_6H_6Cr(CO)_3$.

When a Mo atom is sandwiched between two $[Mo_3S_4]^{4+}$ ligands, forming a $\{[Mo_3S_4]_2Mo\}^{8+}$ cluster cation, the six vacant d^2sp^3 hybridized AOs of the central Mo atom match perfectly the six three-centred two-electron Mo–S–Mo π bonds of the two $[Mo_3S_4]^{4+}$ ligands to form six $L(\pi)\rightarrow M$ bonds, as in the case of $(C_6H_6)_2Cr$. There is, on the other hand, some back-donation of electrons from the central Mo atom to the ligands, somewhat similar to the $M\rightarrow L$ backward bonding (see figure 13). In the case of the half-sandwich complex $\{[Mo_3S_4]Ni\}^{4+}$, the 'intruder' Ni atom provides three vacant sp^3 hybridized AOs to accept three pairs of electrons from the three Mo–S–Mo π bonds of the ligand $[Mo_3S_4]^{4+}$ forming three $[Mo_3S_4]^{4+}\rightarrow M$ bonds. There are, however, five lone pairs of electrons localized on the five 3d AOs of the Ni atom, two lone pairs of which donate significantly backward to the $[Mo_3S_4]^{4+}$ ligand to form an $M\rightarrow[Mo_3S_4]^{4+}$ backward bonding (see figure 15). For the cluster ion

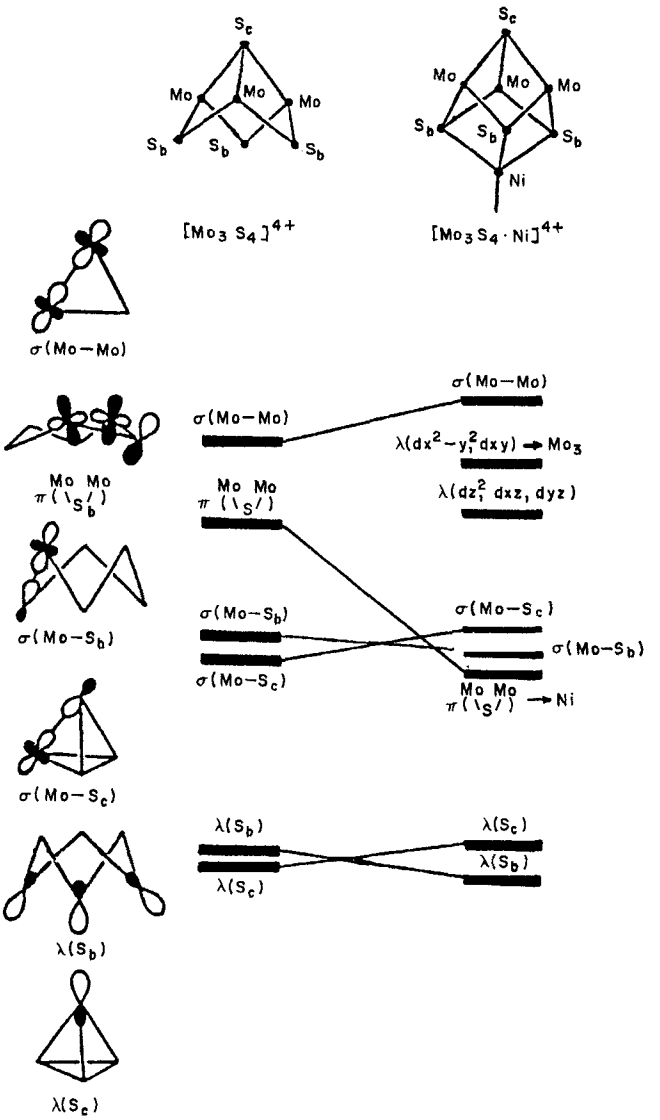

Figure 15. Energy levels of the LMOs of the $[Mo_3S_4\cdot Ni]^{4+}$ cluster core.

$\{[Mo_3S_4]Cu\}^{5+}$, as in the case of $\{[Mo_3S_4]Ni\}^{4+}$, three $[Mo_3S_4]^{4+} \rightarrow M$ bonds are formed with the Cu atom contributing three vacant sp^3 hybridized AOs, thus interacting with the three occupied three-centred two-electron π bonds in the ligand $[Mo_3S_4]^{4+}$. However, the five lone pairs of d electrons localized entirely in the five 3d AOs of the Cu atom without any back donation of electrons to the ligand $[Mo_3S_4]^{4+}$ due to the stabilization of the completely filled 3d AOs of the Cu atom. Finally, in the

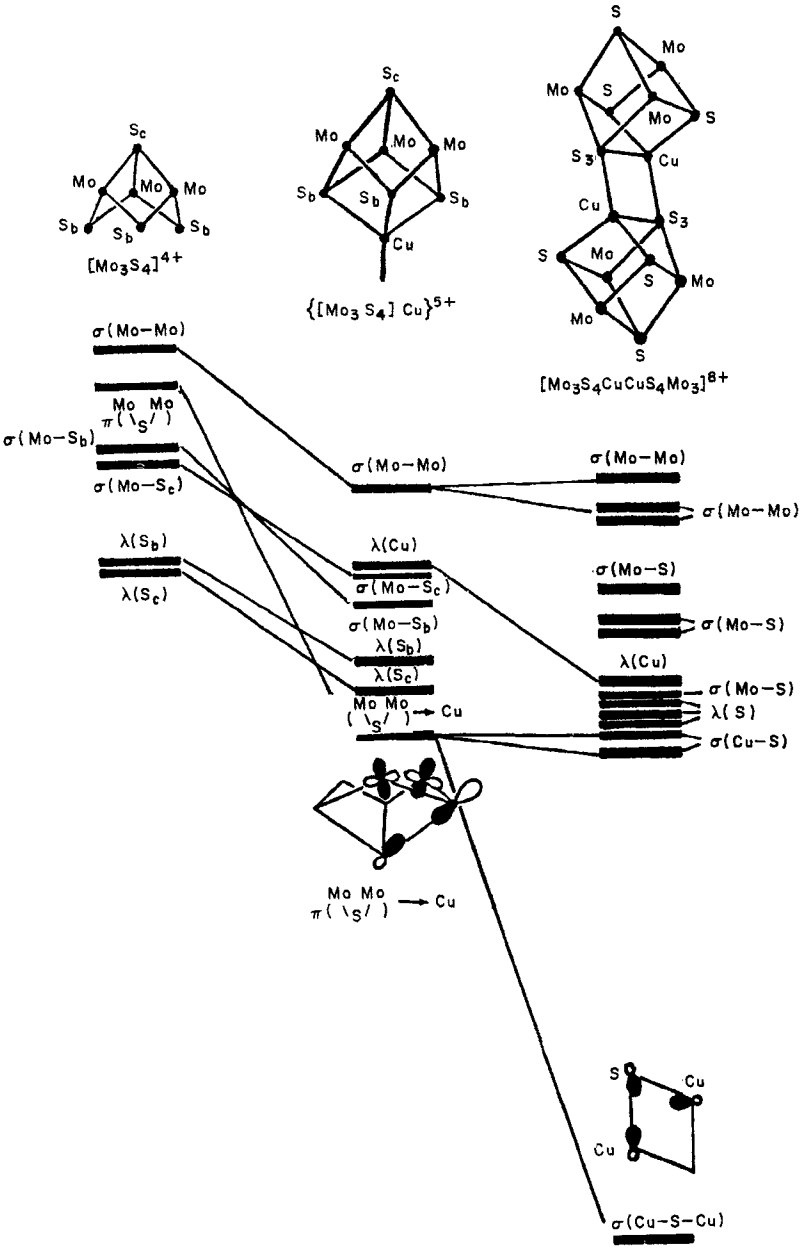

Figure 16. Energy levels of the LMOs of $\{[Mo_3S_4]Cu\}^{5+}$ and $[Mo_3S_4CuCuS_4Mo_3]^{8+}$ cluster cores.

case of $\{[Mo_3S_4]CuCu[S_4Mo_3]\}^{8+}$, two three-centred two-electron σ(Cu–S–Cu) bonds and four σ(Cu–S) bonds are formed, instead of the three $[Mo_3S_4]^{4+} \rightarrow Cu$ bonds in the case of $\{[Mo_3S_4]Cu\}^{5+}$. The ligand $[Mo_3S_4]^{4+}$ loses in this case the initial π-type LMOs, different from the case of the half-sandwich type complex $\{[Mo_3S_4]Cu\}^{5+}$ (see figure 16). In the meanwhile, the five lone pairs of d electrons are again still localized on the five 3d AOs of each Cu atom.

It is interesting that on account of the formation of the $L(\pi) \rightarrow M$ bond, the three three-centred two-electron π bonds in the ligand itself are somewhat weakened; both the C–C bonds in the arene ligand and the Mo–S bonds in the $[Mo_3S_4]^{4+}$ ligand are slightly longer than the corresponding bond lengths in the parent molecule and ion. The 1·398 Å C–C bond distance in the parent molecule C_6H_6 is lengthened to 1·423 Å in $(C_6H_6)_2Cr$, and to 1·423 Å and 1·406 Å in the case of $C_6H_6Cr(CO)_3$ corresponding respectively ligands eclipsed and staggered with respect to the CO ligands [44]. It is interesting to note that the parent quasi-aromatic ligand $[Mo_3S_4]^{4+}$ has shorter bond distance between the bridging S_b and Mo atom than between the capping S_c and Mo atom, and thus, as soon as the 'intruder' metal atom is sandwiched between the $[Mo_3S_4]^{4+}$ ligands with formation of new $L(\pi) \rightarrow M$ bonds, the Mo–S_b bond distances are remarkably lengthened, closer to the Mo–S_c bond length (table 9), whereas the Mo–Mo bond lengths are also slightly increased.

Shibahara [37 (*g*)] has recently suggested that there are two types of driving forces for the formation of sandwich and half-sandwich type mixed-metal clusters from the nido-cubane-type ion $[Mo_3S_4]^{4+}$ and the metal atom, namely reducing ability of the metal and affinity of metal toward bridging S atoms. It seems obvious that the two bonding factors rather resemble the two kinds of bonds between $[Mo_3S_4]^{4+}$–M in which the $L(\pi) \rightarrow M$ bonding behaves as the affinity of metal to S atom, while the backward donation bond $M \rightarrow L$ from the metal to the ligand plays a reductive role for the Mo atoms in the $[Mo_3S_4]^{4+}$ ligand. Therefore a study of the addition reactions of various metals to quasi-aromatic ligand $[M_3(\mu_3\text{–}X)(\mu\text{–}Y)_3]^{4+}$ (M = Mo, W; X, Y = O, S, Se, Te) must be a very interesting subject.

6. Conclusions

In summarizing our work on such an interesting phenomenon of quasi-aromaticity, we would like to remark that it is reasonable for us to regard the puckered $[M_3Y_3]$ six-membered rings in certain discrete trinuclear metal cluster compounds with $[M_3(\mu_3\text{–}X)(\mu_2\text{–}Y)_3]^{4+}$ (M = Mo, W; X, Y = O, S) cores as a novel type of aromatic compounds in transition metal cluster chemistry. The energy-localized MOs analysis leads us, indeed, to a clear-cut quantum-chemical picture for this type of cluster compounds, quite similar to that of benzene insofar as in either of them there exists a closed, completely continuous conjugated π-electron system, formed from the three cooperating three-centred two-electron π bonds, which is a (p–p–p)π conjugated system in the benzene molecule, but a (d–p–d)π one for these cluster compounds. Furthermore, the formation conditions of a closed, completely continuous π-conjugated system in these $[M_3Y_3]$ rings, to our knowledge, are: (1) the appropriate overlaps and the differences in electronegativity between the M and Y atoms lead to delocalize the lone pair electrons from the bridging Y atom to the vacant valence orbitals of the two adjoining metal atoms to form a three-centred two-electron π bond; (2) the inter-π-bonds overlaps to a great extent give rise to a large inter-π-bonds interaction energy, forming a large closed π-conjugated system around the ring, for example, in the case of $[Mo_3S_4]^{4+}$ each pair of adjoining three-centred two-electron

(Mo–S–Mo) π bonds shares the same d AO of the common Mo atom, giving rise to great inter-π-bonds overlaps and forming a large three-dimensional closed, completely continuous π-conjugated system. (3) The appropriate oxidation states of metal atoms and spin electron configurations of the cluster compounds to provide suitable AOs on the metal atoms to accommodate delocalization electrons from the bridging atoms.

Current efforts in our laboratory are directed toward the extension of the $[M_3(\mu_3\text{–}X)(\mu_2\text{–}Y)_3]^q$ series, including both pre- and post-transition metal elements M, and other structural types of transition metal cluster compounds.

Acknowledgments

The authors gratefully acknowledge the support of our quasi-aromaticity research by the National Sciences Foundation of China and the State Key Laboratory of Structural Chemistry. We are grateful to Professors Q.-E. Zhang, C.-W. Liu and J.-Q. Huang for their helpful discussions.

References

[1] (*a*) GARRATT, P. J., 1986, *Aromaticity* (New York: Wiley); (*b*) BALABAN, A. T., 1980, *Pure appl. Chem.*, **52,** 1409; (*c*) 1982, **54,** 1075; (*d*) DEWAR, M. J. S., *et al.*, 1980, *Ibid.*, **52,** 1431; (*e*) 1986, **58,** 67; (*f*) GIMARC, B., *et al.*, 1980, *Ibid.*, **52,** 1443; (*g*) 1990, **62,** 423; (*h*) BOCK, H., 1990, *Ibid.*, **62, 383;** (*i*) HUNIG, S., 1990, *Ibid.*, **62,** 395; (*j*) TODA, F., 1990, *Ibid.*, **62,** 407; (*k*) HARADA, Y., 1990, *Ibid.*, **62,** 457; (*l*) BRYCE, M. R., and MOORE, A. J., 1990, *Ibid.*, **62,** 473; (*m*) BOEKELHEIDE, V., 1986, *Ibid.*, **58,** 1; (*n*) Oda, M., 1986, *Ibid.*, **58,** 7; (*o*) NOBES, R. H., and RADOM, L., 1986, *Ibid.*, **58,** 75; (*p*) MULLER, K., 1986, *Ibid.*, **58,** 177; (*q*) FLITSCH, W., 1986, *Ibid.*, **58,** 153; (*r*) VOGEL, E., 1982, *Ibid.*, **54,** 1015; (*s*) WUDL, F., 1982, *Ibid.*, **54,** 1051; (*t*) SCHAAD, L. J., and HESS, JR., B. A., 1986, *Ibid.*, **54,** 1097.

[2] KROTO, H. W., ALLAF, A. W., and BALM, S. P., 1991, *Chem. Rev.*, **91,** 1213.

[3] HÜCKEL, E., 1938, *Grundzuge der Theorie Ungesattigter und Aromatischer Verbindungen* (Berlin: Velag Chemie).

[4] (*a*) PAULING, L., 1960, *The Nature of the Chemical Bond* (Cornell University Press); (*b*) WHELAND, G. W., 1955, *Resonance in Organic Chemistry* (New York: Wiley); (*c*) INGOLD, C. K., and INGOLD, E. H., 1926, *J. chem. Soc.*, 1310; (*d*) DEWAR, M. J. S., 1969, *The Molecular Orbital Theory of Organic Chemistry* (New York: McGraw-Hill).

[5] MÜLLER, A., JOSTES, R., and COTTON, F. A., 1980, *Angew. Chem. Int. Ed. Engl.*, **19,** 875.

[6] BURSTEN, B. E., COTTON, F. A., HALL, M. B., and NAJJAR, R. C., 1982, *Inorg. Chem.*, **21,** 302.

[7] COTTON, F. A., 1986, *Polyhedron*, **5,** 3.

[8] COLTON, R., 1988, *Coord. Chem. Rev.*, **90,** 29.

[9] SHIBAHARA, T., AKASHI, H., NAGAHATA, S., HATTORI, H., and KUROYA, H., 1989, *Inorg. Chem.*, **28,** 362, and refs. cited.

[10] SHIBAHARA, T., and YAMASAKI, M., 1991, *Inorg. Chem.*, **30,** 1687, and refs. cited.

[11] COTTON, F. A., and FENG, X. J., 1991, *Inorg. Chem.*, **30,** 3666.

[12] (*a*) HUANG, J.-Q., HUANG, J.-L., SHANG, M.-Y., LU, S.-F., LIN, X.-T., LIN, Y.-H., HUANG, M.-D., ZHUANG, H.-H., and LU, J.-X., 1987, *Jiegou Huaxue*, **6,** 219 (in Chinese); (*b*) 1988, *Pure appl. Chem.*, **60,** 1185.

[13] LU, J.-X., 1989, *Jiegou Huaxue*, **8,** 327 (in Chinese).

[14] (*a*) CHEN, Z.-D., LI, J., LIU, C.-W., ZHANG, Q.-E., and LU, J.-X., 1990, *Chinese Science Bulletin*, **35,** 1698; (*b*) 1991, *Prog. Nat. Sci.*, **1,** 33; (*c*) 1991, *Ibid.*, **1,** 133; (*d*) 1991, *Chinese J. Chem.*, **9,** 385; (*e*) CHEN, Z.-D., LU, J.-X., LIU, C.-W., and ZHANG, Q.-E., 1991, *J. Molec. Struct.*, **236,** 343; (*f*) 1991, *Polyhedron*, **10,** 2799.

[15] EDMISTON, C., and RUEDENBERG, K., 1963, *Rev. Mod. Phys.*, **35,** 457.

[16] RUEDENBERG, K., 1971, *Modern Quantum Chemistry*, Part I, edited by O. Sinanoglu (New York: Academic).

[17] BOYS, S. F., 1960, *Rev. Mod. Phys.*, **32,** 296.

[18] LIPSCOMB, W. N., 1975, *Boron Hydride Chemistry*, edited by E. L. Muetterties (New York: Academic), pp. 39–78.

[19] DEWAR, M. J. S., LUCKEN, E. A. C., and WHITEHEAD, M. A., 1960, *J. Chem. Soc.*, 2423.

[20] HALGREN, T. A., BROWN, L. D., KLEIER, D. A., and LIPSCOMB, W. N., 1977, *J. Am. Chem. Soc.*, **99,** 6793.
[21] BHATTACHARJEE, S., KAR, T., and SANNIGRAHI, A. B., 1985, *Indian J. Chem.* A, **24,** 276.
[22] WHEELER, R. A., HOFFMANN, R., and STRAHLE, J., 1986, *J. Am. Chem. Soc.*, **108,** 5381.
[23] CRAIG, D. P., and PADDOCK, N. L., 1962, *J. Chem. Soc.*, 4118.
[24] WU, X.-T., ZHAN, H.-Q., ZHENG, Y.-F., ZHU, L.-Y., CHEN, W.-Z., and LU, J.-X., 1991, Abstracts, *second Chinese Symposum on the Metal Cluster Compounds*, Fuzhou, China, pp. 64–65.
[25] LI, J., 1992, Doctoral Thesis, Fujian Institute of Research on the Structure of Matter, Chinese Academy of Sciences.
[26] BINO, A., COTTON, F. A., and DORI, Z., 1978, *J. Am. Chem. Soc.*, **100,** 5252.
[27] RODGERS, K. R., MURMANN, R. K., SCHLEMPER, E. O., and SHELTON, M. E., 1985, *Inorg. Chem.*, **24,** 1313.
[28] SEGAWA, M., and SASAKI, Y., 1985, *J. Am. Chem. Soc.*, **107,** 5565.
[29] SHIBAHARA, T., TAKEUCH, A., OHTSUJI, A., KOHDA, K., and KUROYA, H., 1987, *Inorg. Chim. Acta*, **127,** L45.
[30] KATHIRGAMANATHAN, P., MARTINEZ, M., and SYKES, A. G., 1985, *J. Chem. Soc. Chem. Commun.*, 1437; 1985, Abstracts, *Fifth International Conference on the Chemistry and Uses of Molybdenum*, p. 133.
[31] SHIBAHARA, T., YAMADA, T., and KUROYA, H., 1986, *Inorg. Chim. Acta*, **113,** L19.
[32] SHIBAHARA, T., HATTORI, H., and KUROYA, H., 1984, *J. Am. Chem. Soc.*, **106,** 2710.
[33] SHIBAHARA, T., MIYAKE, H., OBAYASHI, K., and KUROYA, H., 1986, *Chem. Lett.*, 139.
[34] LU, S.-F., SHANG, M.-Y., HUANG, J.-Q., HUANG, J.-L., and LU, J.-X., 1988, *Sci. Sin*, B, **31,** 147.
[35] LIN, X.-T., LIN, Y.-H., HUANG, J.-L., and HUANG, J.-Q., 1987, *Kexue Tongbao*, **32,** 810.
[36] KOBAYASHI, H., SHIBAHARA, T., and URYU, N., 1990, *Bull. Chem. Soc. Japan*, **63,** 799.
[37] SHIBAHARA, T., *et al.*, (*a*) 1986, *J. Am. Chem. Soc.*, **108,** 1342; (*b*) 1986, *Inorg. Chim. Acta*, **116,** L25; (*c*) 1987, *J. Am. Chem. Soc.*, **109,** 3495; (*d*) 1988, *Coord. Chem.*, **18,** 233; (*e*) 1988, *J. Am. Chem. Soc.*, **110,** 3313; (*f*) 1989, *Inorg. Chem.*, **28,** 2906; (*g*) 1991, *Inorg. Chem.*, **30,** 2693; (*h*) 1991, *Chem. Lett.*, 689.
[38] LU, S.-F., ZHU, N. Y., WU, X.-T., and LU, J.-X., 1989, *J. Molec. Struct.*, **197,** 15.
[39] LU, S.-F., HUANG, J.-Q., LIN, Y.-H., and HUANG, J.-L., 1987, *Acta Chimica Sinica.*, **3,** 199.
[40] OOI, B. L., and SYKES, A. G., 1989, *Inorg. Chem.*, **28,** 3799.
[41] LU, S.-F., HUANG, J.-Q., LIN, Y.-H., and HUANG, J.-L., 1987, *Huaxue Xuebao*, **45,** 666.
[42] WU, X.-T., LU, S.-F., ZHU, L.-Y., WU, Q.-J., and LU, J.-X., 1987, *Inorg. Chim. Acta*, **133,** 39.
[43] DEEG, A., KECK, H., KRUSE, A., KUCHEN, W., and WUNDERLICH, H., 1988, *Z. Naturf.* B, **43,** 1541.
[44] MUETTERTIES, E. L., BLEEK, J. R., and WUCHERER, E. J., 1982, *Chem. Rev.*, **82,** 499.